

Supporting Information

Synthesis of dinuclear pyridyl-amido hafnium and zirconium complexes toward olefin polymerization with unexpected stereospecificity and ultra-high molecular weight capability

Yanhong Xing,^a Shaofeng Liu,^{*.a} and Zhibo Li^{*.a,b}

^a Key Laboratory of Biobased Polymer Materials, College of Polymer Science and Engineering, Qingdao University of Science and Technology, Qingdao, 266042, China

^b College of Chemical Engineering, Qingdao University of Science and Technology, Qingdao, 266042, China

*E-mail: shaofengliu@qust.edu.cn (S.L.); zbli@qust.edu.cn (Z.L.)

Experimental Section

1. General Considerations.	S6
2. Synthesis of Bifunctional Ligand <i>syn-L</i> and Monofunctional Ligand <i>mono-L</i> . ..	S7
3. Synthesis of Hafnium and Zirconium Complexes.	S9
4. General Procedure for Ethylene or Propylene Homopolymerization.	S12
5. General Procedure for Ethylene/1-Octene Copolymerization.	S12
6. Crystal Structure Determinations.	S13
Fig. S1. ¹ H NMR spectrum of <i>syn-L</i> in CDCl ₃	S14
Fig. S2. ¹³ C NMR spectrum of <i>syn-L</i> in CDCl ₃	S14
Fig. S3. ¹ H NMR spectrum of <i>mono-L</i> in CDCl ₃	S15
Fig. S4. ¹³ C NMR spectrum of <i>mono-L</i> in CDCl ₃	S15
Fig. S5. ¹ H NMR spectrum of <i>syn-Hf2</i> in C ₆ D ₆	S16
Fig. S6. ¹³ C NMR spectrum of <i>syn-Hf2</i> in C ₆ D ₆	S16
Fig. S7. ¹ H– ¹ H COSY NMR spectrum of <i>syn-Hf2</i> in C ₆ D ₆	S17
Fig. S8. ¹ H– ¹³ C HSQC NMR spectrum of <i>syn-Hf2</i> in C ₆ D ₆	S17
Fig. S9. ¹ H NMR spectrum of crude product <i>syn-Hf2</i> in C ₆ D ₆	S18
Fig. S10. ¹ H NMR spectrum of <i>syn-Zr2</i> in C ₆ D ₆	S18
Fig. S11. ¹³ C NMR spectrum of <i>syn-Zr2</i> in C ₆ D ₆	S19
Fig. S12. ¹ H NMR spectrum of <i>mono-Hf1</i> in C ₆ D ₆	S19
Fig. S13. ¹³ C NMR spectrum of <i>mono-Hf1</i> in C ₆ D ₆	S20
Fig. S14. ¹ H NMR spectrum of <i>Me-Hf1</i> in C ₆ D ₆	S20
Fig. S15. ¹³ C NMR spectrum of <i>Me-Hf1</i> in C ₆ D ₆	S21
Fig. S16. ¹ H NMR spectrum of <i>Ar-Hf1</i> in C ₆ D ₆	S21
Fig. S17. GPC curve of polyethylene sample obtained in Table 1 run 1.	S22
Fig. S18. GPC curves of polyethylene samples obtained in Table 1 runs 2–5.	S22
Fig. S19. GPC curves of polyethylene samples obtained in Table 1 runs 2, 6–7.	S22
Fig. S20. GPC curves of polymers prepared by <i>syn-Hf2</i> , <i>mono-Hf1</i> , <i>Me-Hf1</i> and <i>Ar-Hf1</i> complexes under otherwise identical conditions (Table 1, runs 4 and 9–11).	S23
Fig. S21. GPC curves of polyethylene samples obtained in Table 1 runs 4 and 12.	S24
Fig. S22. GPC curve of polyethylene sample obtained in Table 1 run 13.	S24

Fig. S23. Stacked ^1H NMR spectra of <i>syn-Hf₂</i> (black), and <i>syn-Hf₂</i> + 1 (red) or 2 (blue) equiv. of $[\text{Ph}_3\text{C}][\text{B}(\text{C}_6\text{F}_5)_4]$ in C_6D_6 .	S25
Fig. S24. Stacked ^1H NMR spectra of <i>syn-Hf₂</i> + 1 (red) or 2 (blue) equiv. of $[\text{Ph}_3\text{C}][\text{B}(\text{C}_6\text{F}_5)_4]$ in CD_2Cl_2 .	S25
Fig. S25. GPC curves of ethylene/1-octene copolymer samples in Table 2 runs 1–3.	S26
Fig. S26. GPC curves of ethylene/1-octene copolymer samples in Table 2 runs 2, 4, and 5.	S26
Fig. S27. GPC curve of ethylene/1-octene copolymer sample in Table 2 run 6.	S27
Fig. S28. GPC curves of ethylene/1-octene copolymer samples in Table 2 runs 2, and 7–9.	S27
Fig. S29. DSC curves of ethylene/1-octene copolymer samples in Table 2 runs 1–3.	S28
Fig. S30. DSC curves of ethylene/1-octene copolymer samples in Table 2 runs 2, 4 and 5.	S28
Fig. S31. DSC curves of ethylene/1-octene copolymer samples in Table 2 runs 2 and 10.	S29
Fig. S32. ^{13}C NMR spectrum of ethylene/1-octene copolymer obtained in Table 2 run 1 in $\text{C}_2\text{D}_2\text{Cl}_4$ at 120 °C (4.0 mol% of 1-octene incorporation).	S29
Fig. S33. ^{13}C NMR spectrum of ethylene/1-octene copolymer obtained in Table 2 run 2 in $\text{C}_2\text{D}_2\text{Cl}_4$ at 120 °C (7.9 mol% of 1-octene incorporation).	S30
Fig. S34. ^{13}C NMR spectrum of ethylene/1-octene copolymer obtained in Table 2 run 3 in $\text{C}_2\text{D}_2\text{Cl}_4$ at 120 °C (12.7 mol% of 1-octene incorporation).	S30
Fig. S35. ^{13}C NMR spectrum of ethylene/1-octene copolymer obtained in Table 2 run 4 in $\text{C}_2\text{D}_2\text{Cl}_4$ at 120 °C (7.9 mol% of 1-octene incorporation).	S31
Fig. S36. ^{13}C NMR spectrum of ethylene/1-octene copolymer obtained in Table 2 run 5 in $\text{C}_2\text{D}_2\text{Cl}_4$ at 120 °C (8.3 mol% of 1-octene incorporation).	S31
Fig. S37. ^{13}C NMR spectrum of ethylene/1-octene copolymer obtained in Table 2 run 6 in $\text{C}_2\text{D}_2\text{Cl}_4$ at 120 °C (5.9 mol% of 1-octene incorporation).	S32

Fig. S38. ^{13}C NMR spectrum of ethylene/1-octene copolymer obtained in Table 2 run 7 in $\text{C}_2\text{D}_2\text{Cl}_4$ at 120 °C (5.7 mol% of 1-octene incorporation).	S32
Fig. S39. ^{13}C NMR spectrum of ethylene/1-octene copolymer obtained in Table 2 run 8 in $\text{C}_2\text{D}_2\text{Cl}_4$ at 120 °C (32.9 mol% of 1-octene incorporation).	S33
Fig. S40. ^{13}C NMR spectrum of ethylene/1-octene copolymer obtained in Table 2 run 9 in $\text{C}_2\text{D}_2\text{Cl}_4$ at 120 °C (37.4 mol% of 1-octene incorporation).	S33
Fig. S41. ^{13}C NMR spectrum of ethylene/1-octene copolymer obtained in Table 2 run 10 in $\text{C}_2\text{D}_2\text{Cl}_4$ at 120 °C (6.6 mol% of 1-octene incorporation).	S34
Fig. S42. GPC curves of polypropylene samples obtained in Table 3 runs 1–3.	S34
Fig. S43. GPC curves of polypropylene samples obtained in Table 3 runs 3 and 4..	S35
Fig. S44. GPC curves of polypropylene samples obtained in Table 3 runs 3, 5 and 6.	S35
Fig. S45. GPC curves of polypropylene samples obtained in Table 3 runs 3, and 7–10.	S36
Fig. S46. DSC curves of propylene polymers obtained in Table 3 runs 3, and 7–10.	S36
Fig. S47. ^{13}C NMR spectrum of PP obtained in Table 3 run 3 in $\text{C}_2\text{D}_2\text{Cl}_4$ at 120 °C (18.8 <i>mmmm</i> %).	S37
Fig. S48. ^{13}C NMR spectrum of PP obtained in Table 3 run 4 in $\text{C}_2\text{D}_2\text{Cl}_4$ at 120 °C (17.2 <i>mmmm</i> %).	S37
Fig. S49. ^{13}C NMR spectrum of PP obtained in Table 3 run 7 in $\text{C}_2\text{D}_2\text{Cl}_4$ at 120 °C (8.2 <i>mmmm</i> %).	S38
Fig. S50. ^{13}C NMR spectrum of PP obtained in Table 3 run 8 in $\text{C}_2\text{D}_2\text{Cl}_4$ at 120 °C (9.6 <i>mmmm</i> %).	S38
Fig. S51. ^{13}C NMR spectrum of PP obtained in Table 3 run 9 in $\text{C}_2\text{D}_2\text{Cl}_4$ at 120 °C (79 <i>mmmm</i> %).	S39
Fig. S52. ^{13}C NMR spectrum of PP obtained in Table 3 run 10 in $\text{C}_2\text{D}_2\text{Cl}_4$ at 120 °C (94 <i>mmmm</i> %).	S39

Fig. S53. Stress-Strain curve for commercial polyolefin elastomer sample (grade: POE/8150, blue) and iPP samples produced by Ar-Hf₁ (black) and Me-Hf₁ (red) at extension rate of 50 mm·min ⁻¹	S40
Table S1. Pentad Distribution and Statistical Analysis for Polypropylene Obtained in Table 3.	S41
Table S2. Crystal Data and Structure Refinement for Metal Complex <i>syn-Hf₂</i>	S42
Table S3. Mechanical Properties of PP samples Produced in Table 3.....	S43
References.....	S44

Experimental Section

1. General Considerations.

All moisture/oxygen sensitive reactions/compounds were performed using standard Schlenk techniques or glovebox techniques in an atmosphere of high-purity N₂. Toluene and *n*-hexane were purified by first purging with dry N₂, followed by passing through columns of activated alumina. 1-Octene was dried by refluxing over sodium under N₂. C₆D₆ were stored over Na/K alloy in vacuo and vacuum transferred immediately prior to use. Ethylene or propylene was purified by passage through a supported MnO oxygen-removal column and an activated Davison 4Å molecular sieve column. The borane B(C₆F₅)₃ and borate [Ph₃C][B(C₆F₅)₄] were purchased from Sigma Aldrich. All other chemicals were purchased from commercial suppliers and used without further purification unless otherwise noted. Reaction temperatures were controlled using an IKA temperature modulator. NMR spectra were recorded on a Bruker AVANCE NEO 400 MHz NMR spectrometer (400 MHz for ¹H NMR and 100 MHz for ¹³C NMR). NMR experiments on air-sensitive samples were conducted in Teflon valve-sealed sample tubes (J. Young). ¹H and ¹³C NMR assays of polymer microstructure were conducted in 1,1,2,2-tetrachloroethane-*d*₂ at 120 °C with a delay time (*d*₁) = 10 seconds. Signals were assigned according to the literature for these polymers.^{1,2} Elemental analyses were performed on the Flash EA 1112 microanalyzer. Gel permeation chromatography (GPC) was carried out in 1,2,4-trichlorobenzene (stabilized with 125 ppm BHT) at 150 °C on the Agilent 1260 infinity II HT GPC instrument equipped with a set of three Agilent PL gel 10 μm mixed-BLS columns with

differential refractive index, viscosity, and light scattering (15 and 90°) detectors. Data reported were determined via triple detection. Molecular weights were determined through universal calibration relative to polystyrene standards. Differential scanning calorimetry (DSC) was performed using a TA differential scanning calorimeter DSC 25 that was calibrated using high purity indium at a heating rate of 10 °C/min. Melting temperatures (T_m) and glass transition temperatures (T_g) were determined from the second scan at a heating rate of 10 °C/min following a slow cooling rate of 10 °C/min to remove the influence of thermal history. An Instron 5943 tensile testing machine was used to characterize the mechanical of elastomers with a span length of 10 mm at a testing speed of 50 mm min⁻¹ at room temperature. Before testing, the samples were tailored into rectangular strips with a width of 4 mm and the thickness was measured separately for each sample. The crystal structure of compression-molded films was studied using wide-angle X-ray diffraction. Fourier transform infrared spectroscopy (FT-IR) was carried out with a Bruker VERTEX70 FT-IR spectrometer. The samples for IR study were prepared as Reflection mode. A WAXS consisted of a computer-controlled wide-angle goniometer coupled to a sealed tube source of Cu-K α radiation operating at 30 KV and 30 mA. The Cu-K α line was filtered using electronic filtering and the usual thin Ni filter. The compounds 1,8-diaminoanthracene,³ 1-aminoanthracene,⁴ and 6-naphthyl-2-pyridinecarboxaldehyde⁵ were prepared according to literature procedures.

2. Synthesis of Bifunctional Ligand *syn-L* and Monofunctional Ligand *mono-L*.

Synthesis of *syn-L*. 1,8-Diaminoanthracene (0.416 g, 2.00 mmol), 6-naphthyl-2-pyridinecarboxaldehyde (1.14 g, 4.40 mmol) and *p*-TsOH (0.010 g) were dissolved in 50 mL methanol. The mixture was allowed to stir for 6 h at room temperature and an orange suspension was obtained. The suspension was filtered to give *syn-L* as an orange powder (1.05 g, 1.64 mmol, 82%). ¹H NMR (400 MHz, CDCl₃): δ 9.64 (s, 1 H), 8.97 (s, 2 H), 8.66 (d, *J* = 7.9 Hz, 2 H), 8.48 (s, 1 H), 8.16 (d, *J* = 9.4 Hz, 2 H), 8.04–7.90 (m, 8 H), 7.78–7.68 (m, 4 H), 7.65–7.57 (m, 2 H), 7.56–7.48 (m, 6 H), 7.21 (d, *J* = 6.2 Hz, 2 H) ppm. ¹³C NMR (100 MHz, CDCl₃): δ 160.95, 159.51, 155.15, 148.74, 138.03, 136.98, 134.14, 132.60, 131.26, 129.35, 128.58, 127.88, 127.71, 126.95, 126.77, 126.66, 126.17, 126.02, 125.96, 125.62, 125.50, 120.16, 119.72, 111.63 ppm. Anal. Calcd for C₄₆H₃₀N₄·1/2MeOH: C, 85.30; H, 4.93; N, 8.56. Found: C, 85.10; H, 4.63; N, 8.67. HRMS Calcd. for [M+H⁺] 639.2547, found 639.2539.

Synthesis of *mono-L*. 1-Aminoanthracene (0.386 g, 2.00 mmol), 6-naphthyl-2-pyridinecarboxaldehyde (0.512 g, 2.20 mmol) and *p*-TsOH (0.010 g) were dissolved in 50 mL methanol. The mixture was allowed to stir for 6 h at room temperature and an orange suspension was obtained. The suspension was filtered to give *mono-L* as a yellow powder (0.95 g, 1.56 mmol, 78%). ¹H NMR (400 MHz, CDCl₃): δ 8.99 (s, 1 H), 8.93 (s, 1 H), 8.61 (d, *J* = 7.8 Hz, 1 H), 8.46 (s, 1 H), 8.16 (d, *J* = 7.3 Hz, 1 H), 8.09 (dd, *J* = 8.6, 4.4 Hz, 2 H), 8.04 (dd, *J* = 9.0, 5.1 Hz, 1 H), 7.98–7.91 (m, 3 H), 7.74 (d, *J* = 7.3 Hz, 1 H), 7.72 (d, 7.3 Hz, 1 H), 7.61 (t, *J* = 7.6 Hz, 1 H), 7.57–7.43 (m, 5 H), 7.15 (d, *J* = 7.0 Hz, 1 H) ppm. ¹³C NMR (100 MHz, CDCl₃): δ 161.29, 159.52, 154.86, 148.69, 138.10, 137.34, 134.17, 132.27, 132.15, 131.79, 131.30, 129.35, 128.88,

128.59, 128.18, 127.93, 127.73, 127.10, 126.81, 126.77, 126.26, 126.17, 125.84, 125.67, 125.62, 125.57, 125.52, 122.95, 120.39, 111.73 ppm. Anal. Calcd for $C_{30}H_{20}N_2 \cdot 1/6MeOH$: C, 87.55; H, 5.03; N, 6.77. Found: C, 87.32; H, 4.85; N, 6.71. HRMS Calcd. for $[M+H^+]$ 409.1705, found 409.1699.

3. Synthesis of Hafnium and Zirconium Complexes.

Synthesis of *syn*-Hf₂. To a suspension of HfCl₄ (0.356 g, 1.10 mmol) in 20 mL toluene was added 1.65 mL MeMgBr solution (4.95 mmol, 3.0 M in ether) using a syringe at $-40\text{ }^\circ\text{C}$. The reaction mixture was stirred at $-40\text{ }^\circ\text{C}$ for 2 h. Then, to this reaction mixture was slowly added a solution of *syn*-**L** (0.319 g, 0.50 mmol) in 30 mL toluene at $-40\text{ }^\circ\text{C}$. The reaction mixture was stirred at $-40\text{ }^\circ\text{C}$ for 2 h and then at room temperature for 12 h to give a dark-yellow suspension. The solvent was removed under reduced pressure. To the residue was added 30 mL toluene, and the suspension was filtered. All the volatiles were removed under vacuum, and the residue was washed by *n*-hexane to give *syn*-**Hf₂** as a yellow powder (0.35 g, 0.32 mmol, 64% yield). ¹H NMR (400 MHz, C₆D₆): δ 8.82 (s, 1 H), 8.43 (d, $J = 7.6$ Hz, 2 H), 8.37 (s, 1 H), 8.06 (d, $J = 8.0$ Hz, 2 H), 7.85 (d, $J = 17.1$ Hz, 2 H), 7.81 (d, $J = 8.1$ Hz, 4 H), 7.56 (d, $J = 6.7$ Hz, 2 H), 7.40–7.28 (m, 6 H), 7.04 (d, $J = 8.0$ Hz, 2 H), 6.24 (d, $J = 7.6$ Hz, 2 H), 6.04 (t, $J = 7.8$ Hz, 2 H), 5.46 (q, $J = 6.6$ Hz, 2 H), 0.90 (d, $J = 6.6$ Hz, 6 H), 0.80 (s, 6 H), 0.27 (s, 6 H) ppm. ¹³C NMR (100 MHz, C₆D₆): δ 205.91, 170.96, 164.12, 144.21, 144.05, 140.40, 135.69, 134.55, 133.61, 130.49, 130.06, 129.65, 129.33, 129.31, 127.08, 126.51, 126.14, 125.85, 125.68, 124.24, 120.27, 120.06, 118.70, 70.18, 63.01, 60.15, 25.23 ppm. Anal. Calcd for C₅₂H₄₆Hf₂N₄: C, 57.62; H, 4.28; N, 5.17. Found: C, 57.59; H, 4.31; N, 5.22.

Synthesis of *syn-Zr₂*. Using the method described for *syn-Hf₂*, *syn-Zr₂* was obtained as an orange powder (0.25 g, 0.28 mmol, 56% yield). ¹H NMR (400 MHz, C₆D₆): δ 8.85 (s, 1 H), 8.48 (d, *J* = 7.6 Hz, 2 H), 8.35 (s, 1 H), 8.10 (d, *J* = 6.8 Hz, 2 H), 7.81–7.75 (m, 6 H), 7.60 (d, *J* = 6.7 Hz, 2 H), 7.39–7.30 (m, 6 H), 7.08 (d, *J* = 8.0 Hz, 2 H), 6.21 (d, *J* = 7.7 Hz, 2 H), 6.07 (t, *J* = 7.8 Hz, 2 H), 5.38 (q, *J* = 6.6 Hz, 2 H), 1.00 (d, *J* = 6.2 Hz, 6 H), 0.43 (s, 6 H), 0.30 (s, 6 H) ppm. ¹³C NMR (100 MHz, C₆D₆): δ 192.40, 170.49, 164.11, 143.77, 142.68, 140.34, 135.81, 134.52, 132.91, 130.05, 129.84, 129.43, 129.34, 128.89, 127.00, 126.86, 126.15, 125.74, 125.65, 124.27, 120.47, 119.93, 118.71, 70.19, 49.49, 46.06, 24.76 ppm. Anal. Calcd for C₅₂H₄₆Zr₂N₄: C, 68.68; H, 5.10; N, 6.16. Found: C, 68.54; H, 4.80; N, 6.06.

Synthesis of *mono-Hf₁*. To a suspension of HfCl₄ (0.356 g, 1.10 mmol) in 20 mL toluene was added 1.65 mL MeMgBr solution (4.95 mmol, 3.0 M in ether) using a syringe at –40 °C. The reaction mixture was stirred at –40 °C for 2 h. Then, to this reaction mixture was slowly added a solution of *mono-L* (0.393 g, 1.00 mmol) in 30 mL toluene at –40 °C. The reaction mixture was stirred at –40 °C for 2 h and then at room temperature for 12 h to give a dark-yellow suspension. The solvent was removed from the reaction mixture under reduced pressure. To the residue was added 70 mL hexane. After it was stirred for 5 min at ambient temperature, the suspension was filtered. The filtrate was concentrated to 5 mL under vacuum, and the mixture was filtered to give *mono-Hf₁* as a yellow powder (0.46 g, 0.73 mmol, 73% yield). ¹H NMR (400 MHz, C₆D₆): δ 8.83 (s, 1 H), 8.49 (d, *J* = 7.6 Hz, 1 H), 8.35 (d, *J* = 8.5 Hz, 1 H), 8.30 (s, 1 H), 7.86–7.75 (m, 3 H), 7.72–7.65 (m, 3 H), 7.60 (d, *J* = 8.0 Hz, 1 H), 7.44–

7.34 (m, 2 H), 7.32–7.28 (m, 1 H), 7.27 (dd, $J = 6.5, 1.2$ Hz, 1 H), 7.25–7.21 (m, 1 H), 6.99 (t, $J = 7.9$ Hz, 1 H), 6.45 (d, $J = 7.7$ Hz, 1 H), 5.63 (q, $J = 6.3$ Hz, 1 H), 1.12 (d, $J = 6.6$ Hz, 3 H), 0.88 (s, 3 H), 0.36 (s, 3 H) ppm. ^{13}C NMR (100 MHz, C_6D_6): δ 206.23, 171.95, 166.17, 144.91, 140.58, 135.82, 134.42, 133.75, 132.28, 132.14, 130.66, 130.09, 129.89, 129.01, 126.97, 126.85, 125.98, 125.72, 125.61, 125.50, 124.16, 123.65, 120.46, 118.59, 63.58, 24.77 ppm. Anal. Calcd for $\text{C}_{33}\text{H}_{28}\text{HfN}_2$: C, 62.81; H, 4.47; N, 4.44. Found: C, 62.75; H, 4.51; N, 4.52.

Synthesis of Me-Hf₁. Using the method described for *mono-Hf₁*, **Me-Hf₁** was obtained as a yellow powder (0.47 g, 0.77 mmol, 77% yield). ^1H NMR (400 MHz, C_6D_6): δ 8.53 (d, $J = 7.6$ Hz, 1 H), 8.29 (d, $J = 8.4$ Hz, 1 H), 7.78 (d, $J = 7.6$ Hz, 1 H), 7.71 (d, $J = 8.1$ Hz, 1 H), 7.52 (d, $J = 8.0$ Hz, 1 H), 7.35–7.19 (m, 5 H), 6.96 (t, $J = 7.9$ Hz, 1 H), 6.46 (d, $J = 7.8$ Hz, 1 H), 4.92 (q, $J = 6.8$ Hz, 1 H), 4.36 (hept, $J = 6.8$ Hz, 1 H), 3.12 (hept, $J = 6.8$ Hz, 1 H), 1.56 (d, $J = 6.8$ Hz, 3 H), 1.39 (d, $J = 6.8$ Hz, 3 H), 1.34 (d, $J = 6.7$ Hz, 3 H), 1.22 (d, $J = 6.8$ Hz, 3 H), 1.13 (d, $J = 6.8$ Hz, 3 H), 0.79 (s, 3 H), 0.64 (s, 3 H) ppm. ^{13}C NMR (100 MHz, C_6D_6): δ 206.23, 171.17, 164.97, 147.29, 146.75, 145.47, 143.82, 140.74, 135.72, 134.29, 130.70, 130.00, 129.77, 126.90, 126.46, 125.47, 125.40, 124.46, 124.11, 120.40, 117.76, 73.15, 66.20, 62.78, 28.62, 27.65, 27.49, 26.56, 25.30, 25.27, 24.90 ppm. Anal. Calcd for $\text{C}_{31}\text{H}_{36}\text{HfN}_2$: C, 60.53; H, 5.90; N, 4.55. Found: C, 60.65; H, 5.93; N, 4.52.

Synthesis of Ar-Hf₁. Using the method described for *mono-Hf₁*, **Ar-Hf₁** was obtained as a yellow powder (0.47 g, 0.77 mmol, 77%). ^1H NMR (400 MHz, C_6D_6): δ 8.60 (d, $J = 7.6$ Hz, 1 H), 8.26 (d, $J = 7.7$ Hz, 1 H), 7.83 (d, $J = 7.6$ Hz, 1 H), 7.74–7.71 (m, 1 H),

7.51 (d, $J = 7.9$ Hz, 1 H), 7.36–7.33 (m, 1 H), 7.32–7.26 (m, 2 H), 7.09–7.06 (m, 2 H), 7.02–6.99 (m, 2 H), 6.82 (t, $J = 7.9$ Hz, 1 H), 6.57 (s, 1 H), 6.56 (d, $J = 7.1$ Hz, 1 H), 3.86 (hept, $J = 6.8$ Hz, 1 H), 3.41 (hept, $J = 6.8$ Hz, 1 H), 2.93 (hept, $J = 6.9$ Hz, 1 H), 1.38 (dd, $J = 6.8, 3.7$ Hz, 6 H), 1.19 (d, $J = 6.7$ Hz, 3 H), 1.15 (d, $J = 7.1$ Hz, 3 H), 0.96 (s, 3 H), 0.71 (s, 6 H), 0.40 (d, $J = 6.7$ Hz, 3 H) ppm. The spectrum of **Ar-Hf1** is consistent with the data reported previously.^{5,6}

4. General Procedure for Ethylene or Propylene Homopolymerization.

In the glovebox, a 350 mL heavy walled glass reactor equipped with a stir bar was loaded with 2 μ mol of mononuclear complex or 1 μ mol of dinuclear complex with 2.4 μ mol of $[\text{Ph}_3\text{C}][\text{B}(\text{C}_6\text{F}_5)_4]$. The glass reactor was then interfaced to a high-pressure line to remove nitrogen and charged three times with ethylene. At the reaction temperature, toluene (30 mL) was introduced by syringe. Then, ethylene at 5 atm pressure was introduced and maintained during the experiments by a continuous feeding. After the desired reaction time, the reactor was vented and 5 mL acidified methanol was syringed in. The contents of the polymerization vessel were poured into a large volume of methanol, and the polymer flakes precipitated out. The resulting polymer was filtered off, washed with methanol, and then dried under vacuum overnight. Propylene homopolymerizations were carried out under otherwise identical conditions, except using propylene instead of ethylene.

5. General Procedure for Ethylene/1-Octene Copolymerization.

In the glovebox, a 350 mL heavy walled glass reactor equipped with a stir bar was loaded with 2 μmol of mononuclear complex or 1 μmol of dinuclear complex with 2.4 μmol of $[\text{Ph}_3\text{C}][\text{B}(\text{C}_6\text{F}_5)_4]$. The glass reactor was then interfaced to a high-pressure line to remove nitrogen and charged three times with ethylene. At the reaction temperature, a mixture of toluene and 1-octene (total volume 30 mL) was introduced by syringe. Then, ethylene at 5 atm pressure was introduced and maintained during the experiments by continuous feeding. After the desired reaction time, the reactor was vented and 5 mL acidified methanol was syringed in. The contents of the polymerization vessel were poured into a large volume of methanol, and the copolymer precipitated out. The resulting copolymer was filtered off, washed with methanol, and then dried under vacuum overnight.

6. Crystal Structure Determinations.

Single crystals of ***syn-Hf₂*** were obtained by recrystallization of its toluene/*n*-hexane solution at $-20\text{ }^\circ\text{C}$. X-ray diffraction study for ***syn-Hf₂*** was carried out on a Bruker D8 Venture diffractometer using graphite-monochromated Mo-K α radiation ($\lambda = 0.71073\text{ \AA}$). Cell parameters were obtained by global refinement of the positions of all collected reflections. Intensities were corrected for Lorentz and polarization effects and empirical absorption. Using Olex2, the structure was solved with the XS and refined with the ShelXL (Sheldrick, 2015).⁷ Crystal data for ***syn-Hf₂*** is summarized in Table S2 in Supporting Information. CCDC reference number 2350275 is for complex ***syn-Hf₂***.

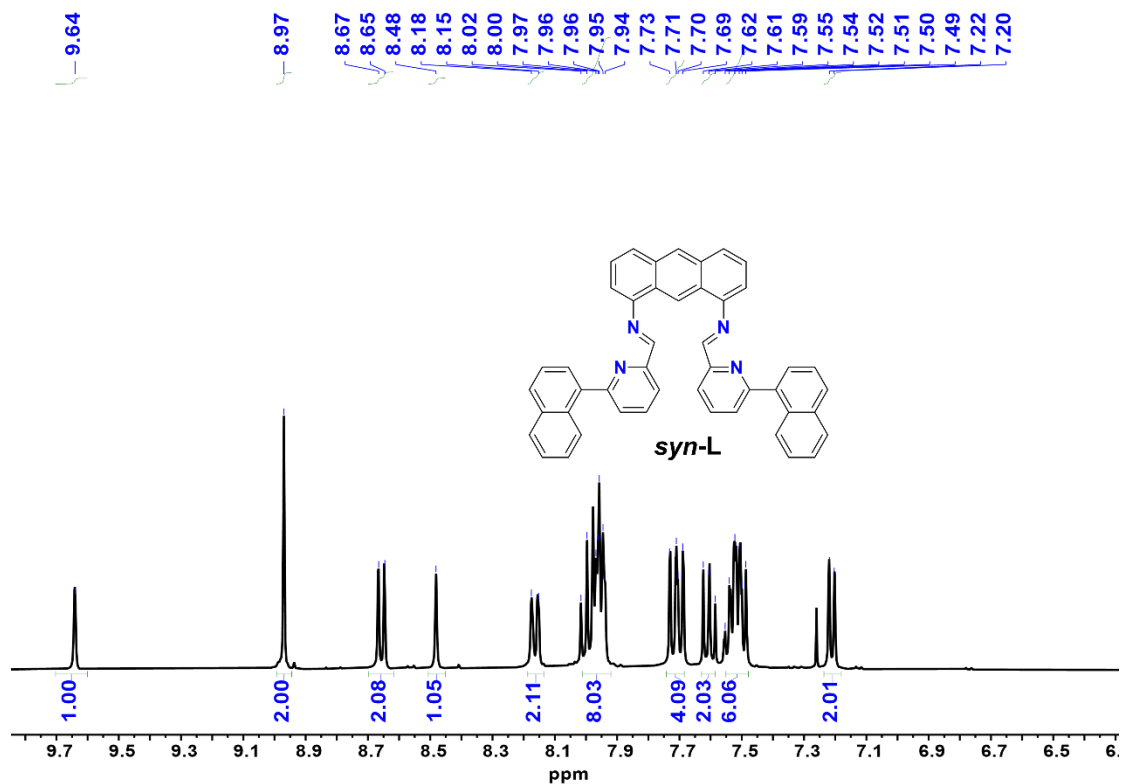


Fig. S1. ¹H NMR spectrum of *syn-L* in CDCl₃.

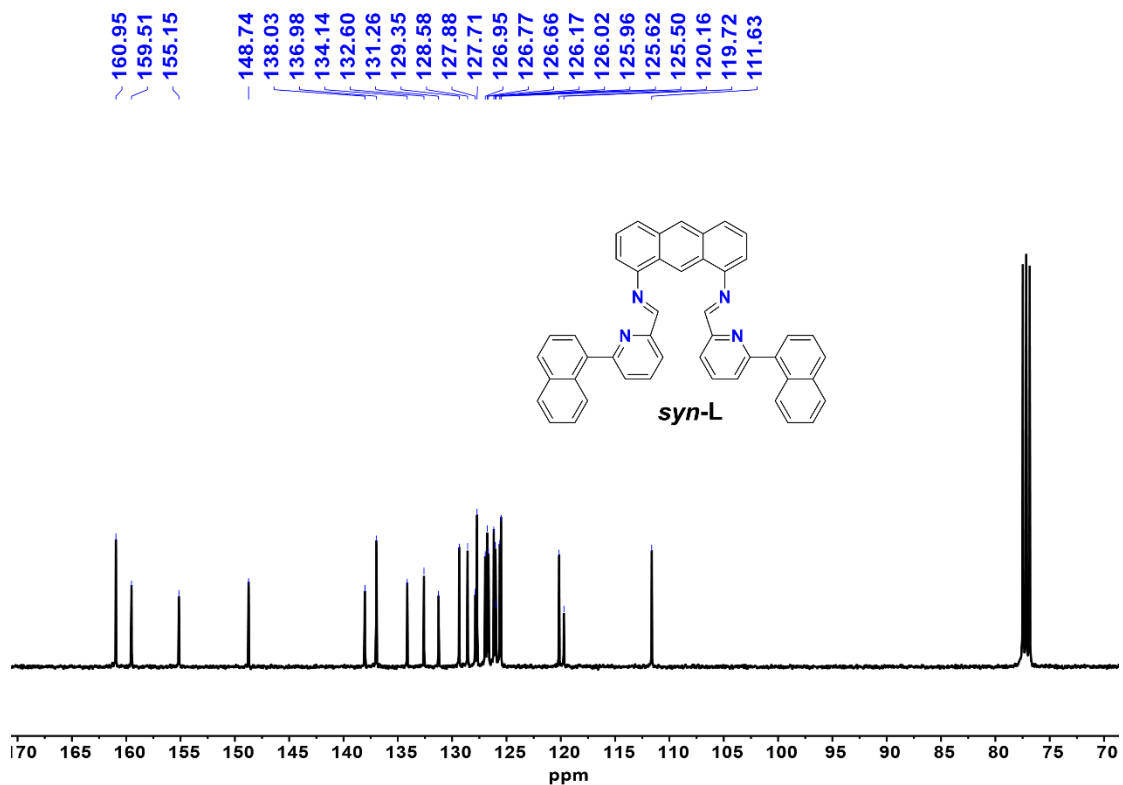


Fig. S2. ¹³C NMR spectrum of *syn-L* in CDCl₃.

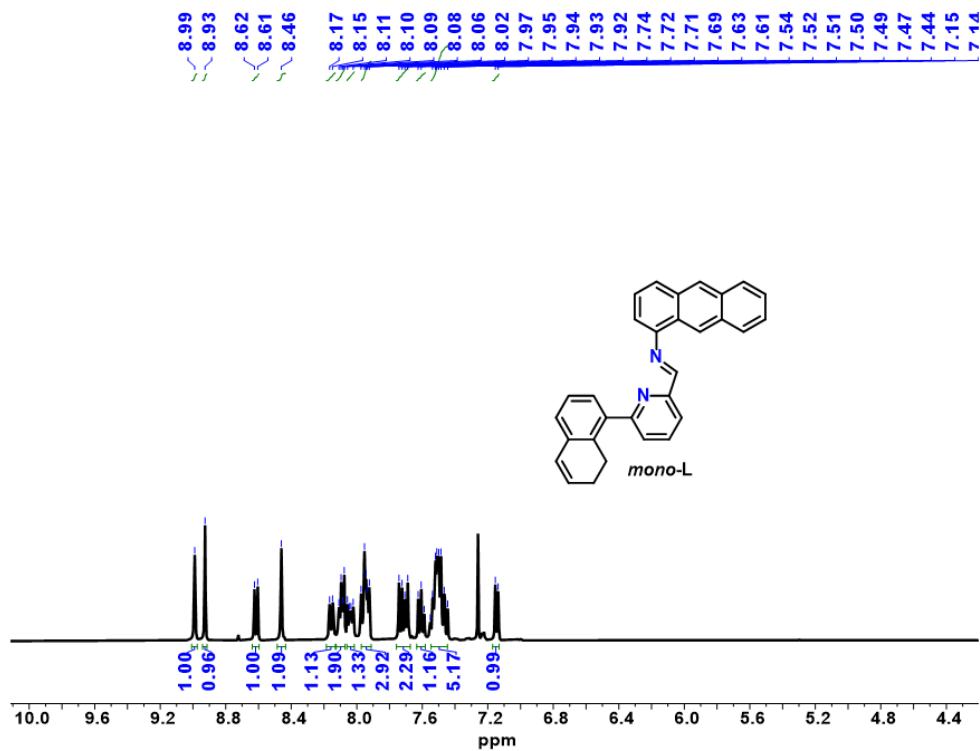


Fig. S3. ¹H NMR spectrum of *mono-L* in CDCl₃.

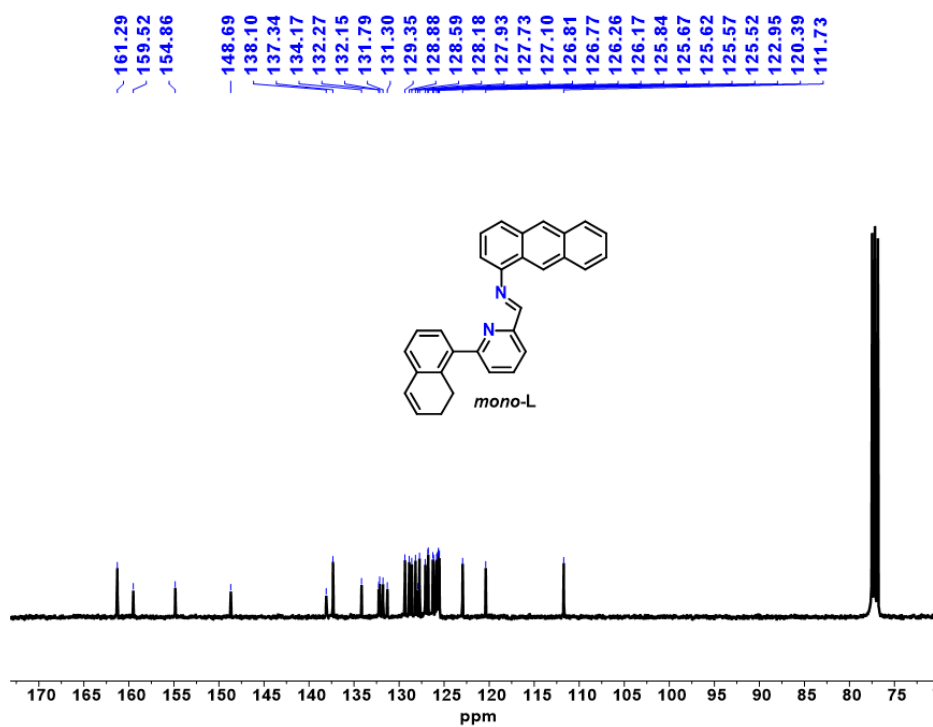


Fig. S4. ¹³C NMR spectrum of *mono-L* in CDCl₃.

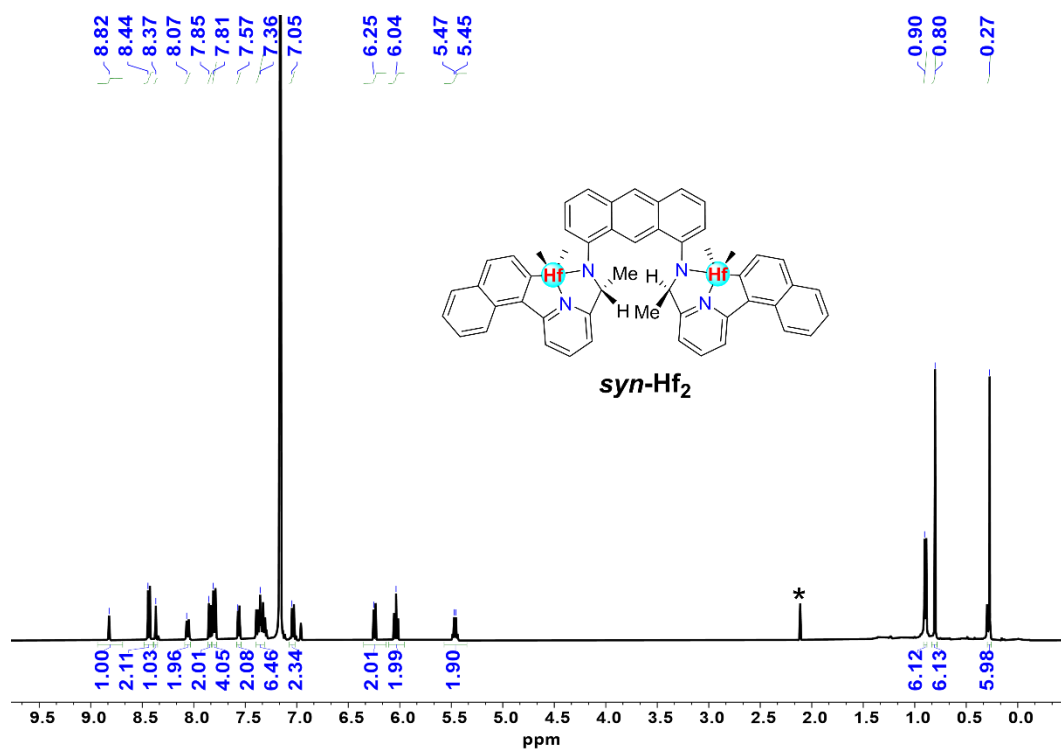


Fig. S5. ¹H NMR spectrum of *syn-Hf₂* in C₆D₆ (* Additional peaks caused by toluene).

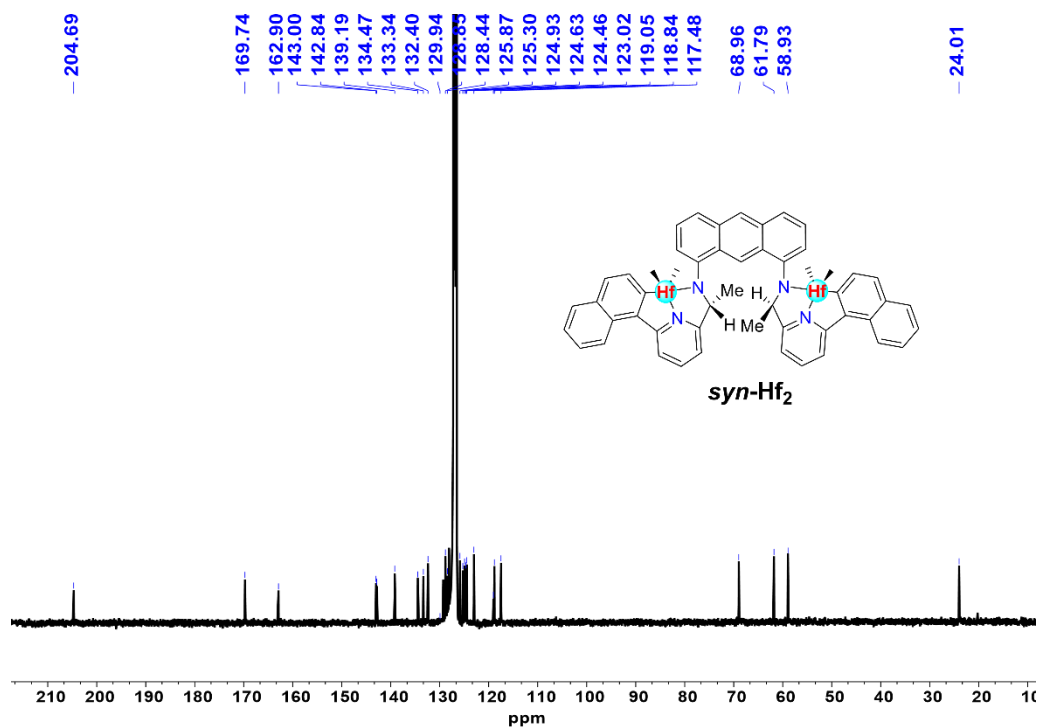


Fig. S6. ¹³C NMR spectrum of *syn-Hf₂* in C₆D₆.

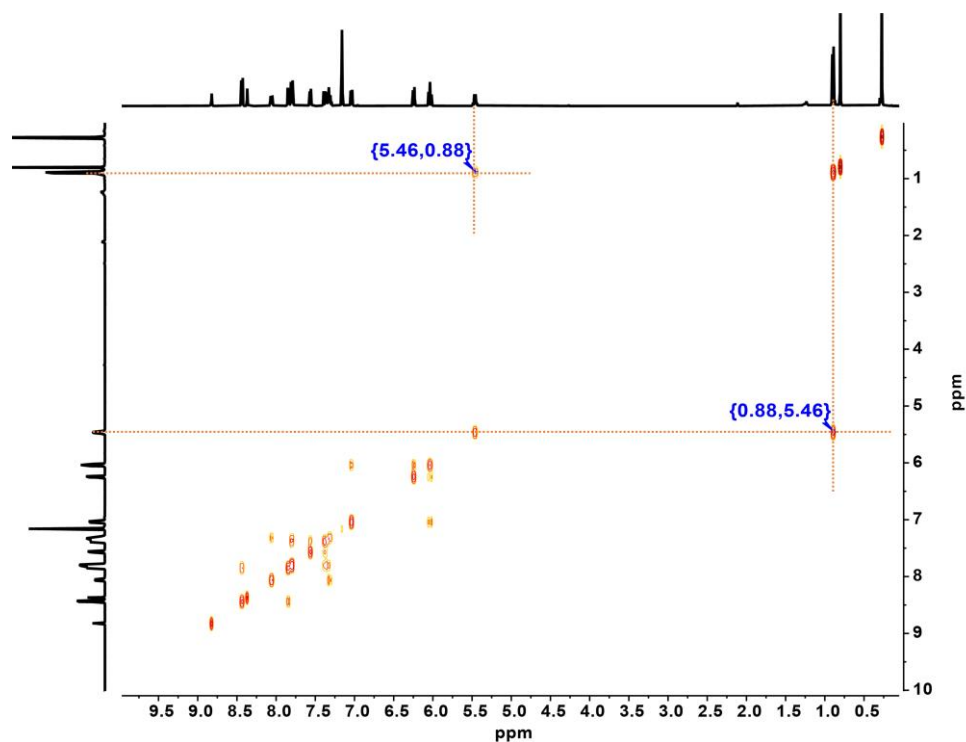


Fig. S7. ^1H - ^1H COSY NMR spectrum of *syn*-**Hf**₂ in C_6D_6 .

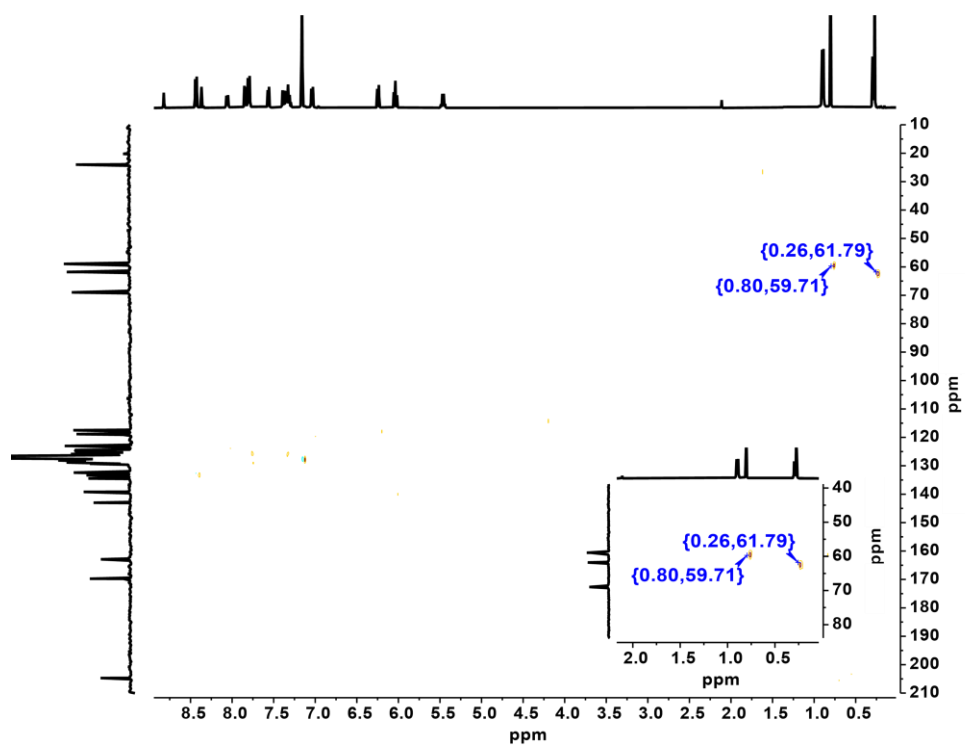


Fig. S8. ^1H - ^{13}C HSQC NMR spectrum of *syn*-**Hf**₂ in C_6D_6 .

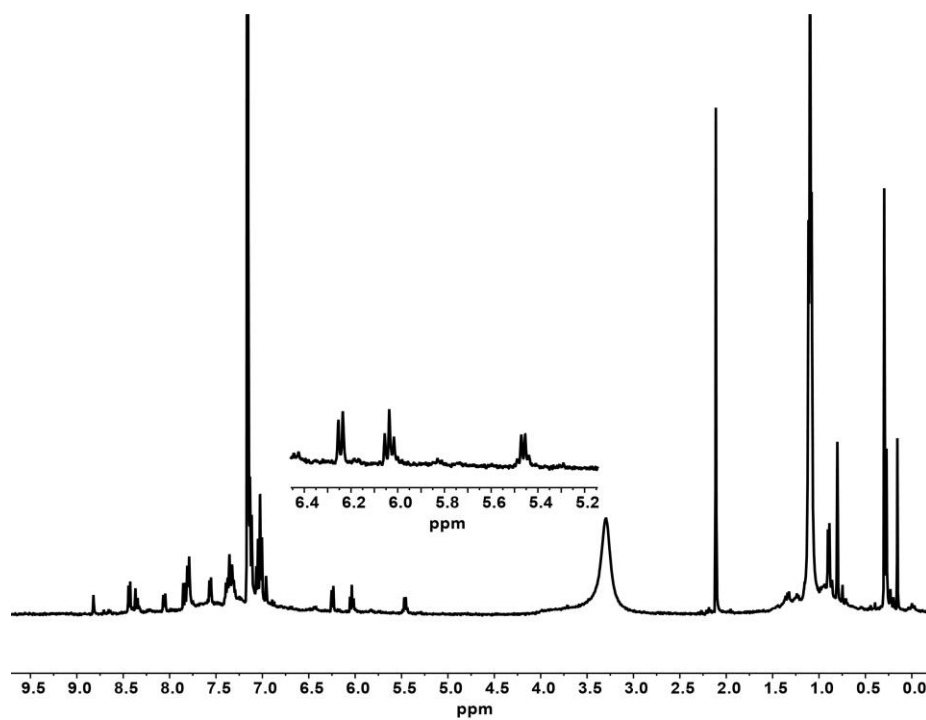


Fig. S9. ^1H NMR spectrum of crude product *syn*- Hf_2 in C_6D_6 .

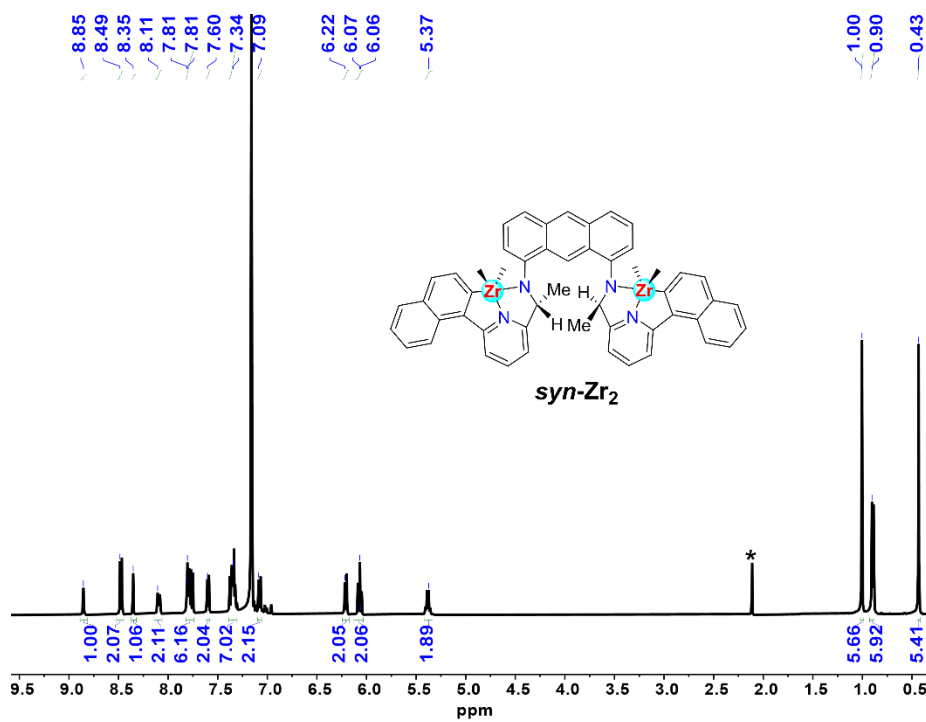


Fig. S10. ^1H NMR spectrum of *syn*- Zr_2 in C_6D_6 (* Additional peaks caused by toluene).

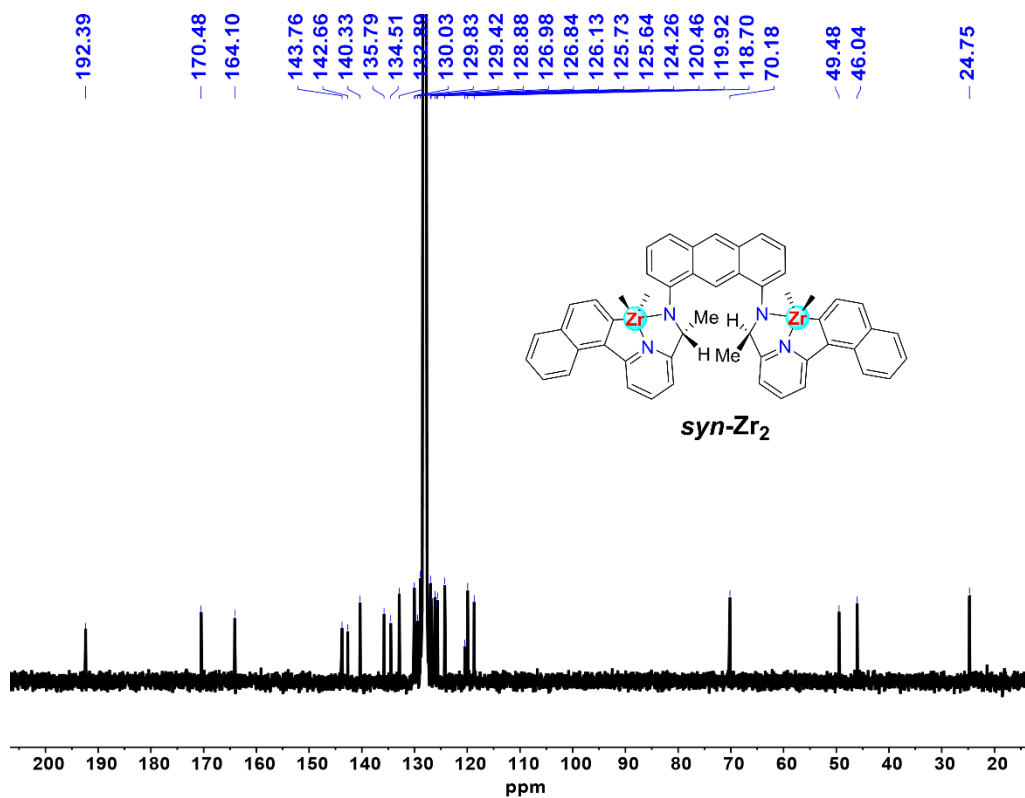


Fig. S11. ¹³C NMR spectrum of *syn-Zr₂* in C₆D₆.

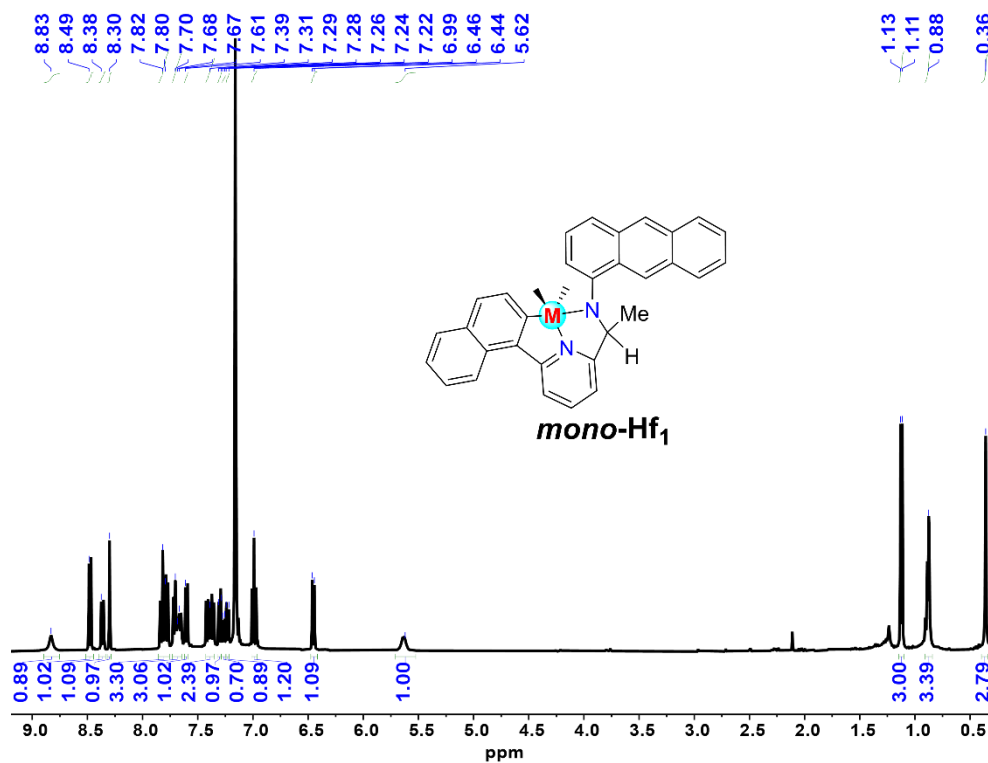


Fig. S12. ¹H NMR spectrum of *mono-Hf₁* in C₆D₆.

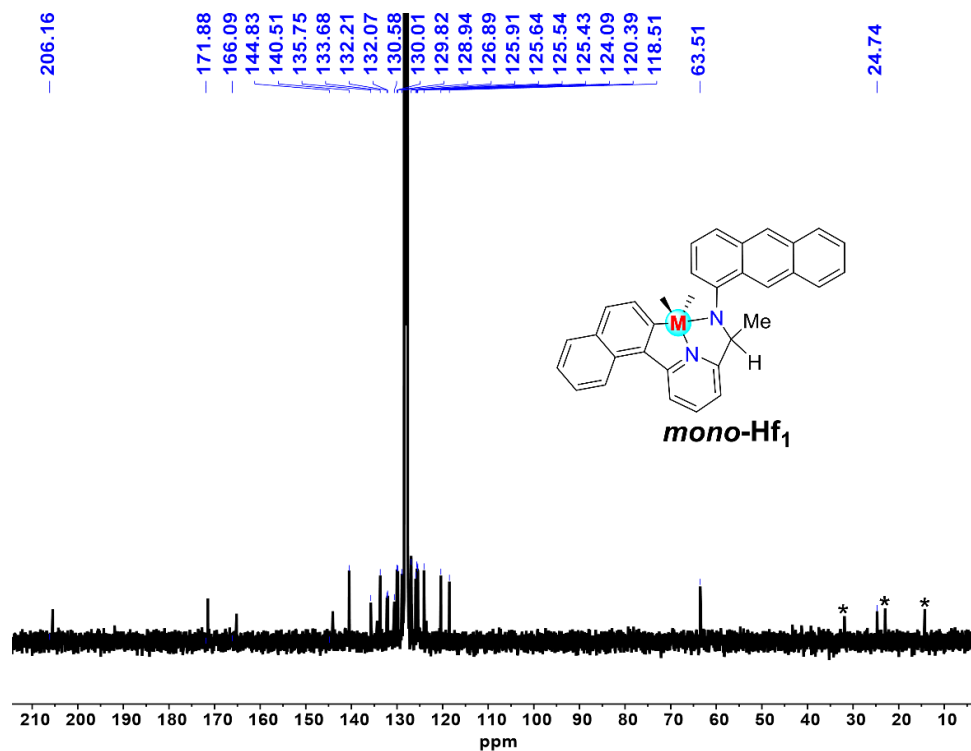


Fig. S13. ¹³C NMR spectrum of *mono-Hf₁* in C₆D₆ (*Additional peaks caused by Hexane).

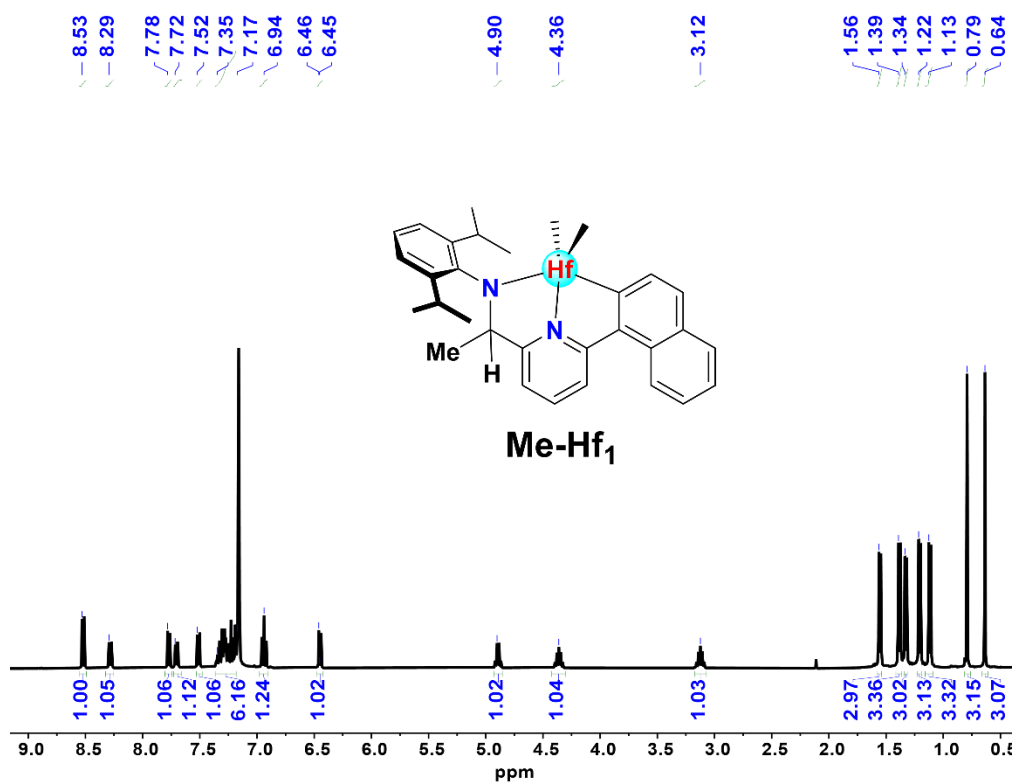


Fig. S14. ¹H NMR spectrum of *Me-Hf₁* in C₆D₆.

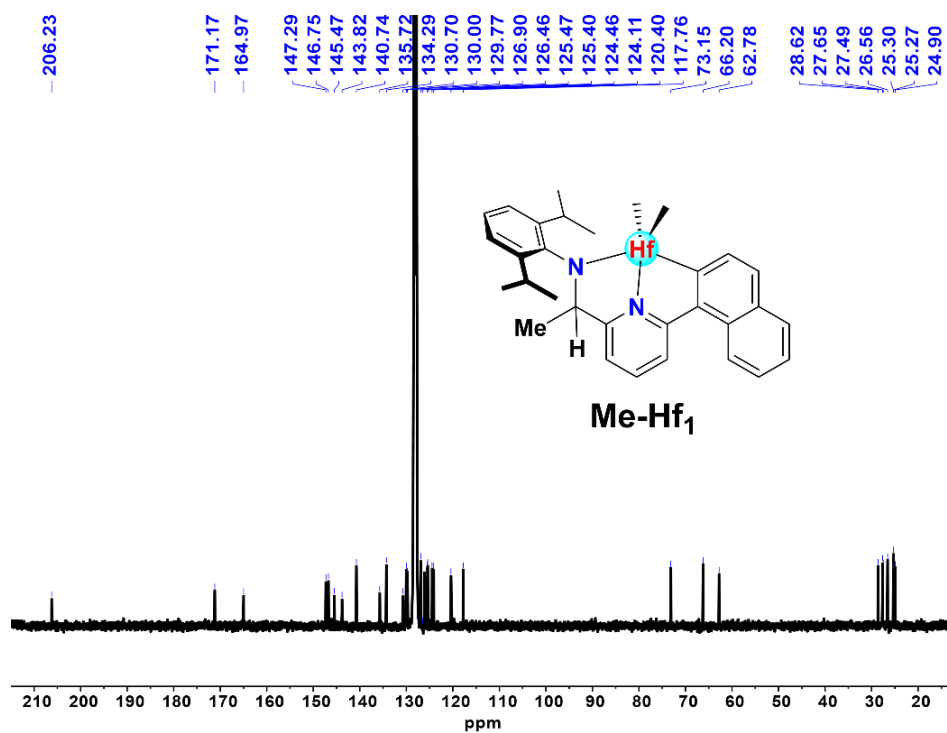


Fig. S15. ¹³C NMR spectrum of Me-Hf₁ in C₆D₆.

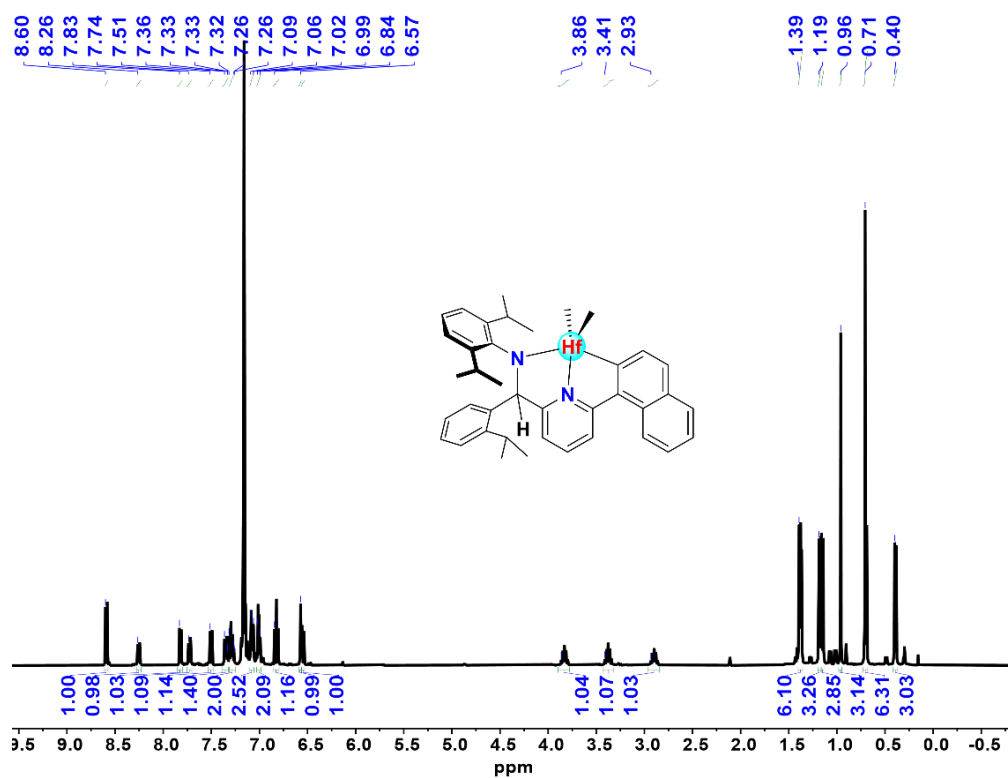


Fig. S16. ¹H NMR spectrum of Ar-Hf₁ in C₆D₆.

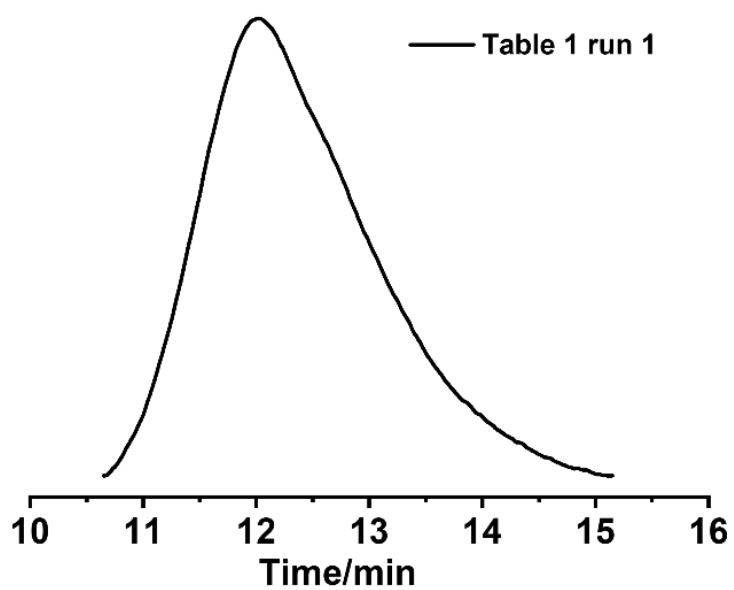


Fig. S17. GPC curve of polyethylene sample obtained in Table 1 run 1.

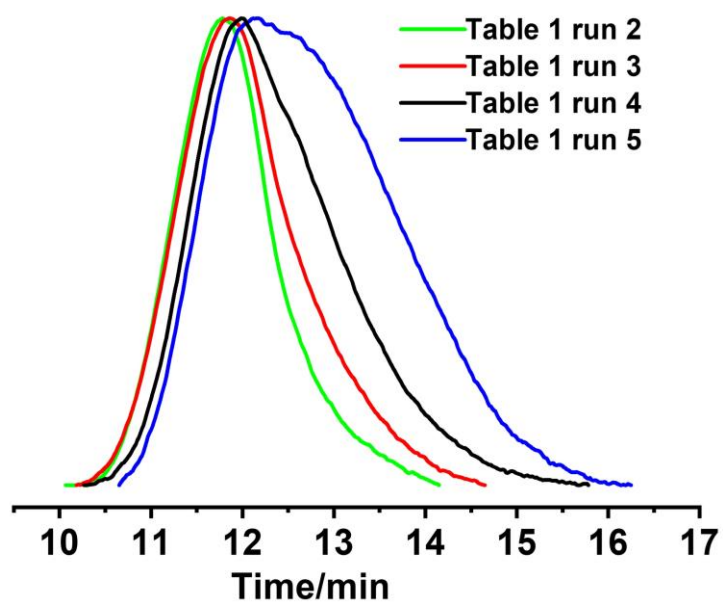


Fig. S18. GPC curves of polyethylene samples obtained in Table 1 runs 2–5.

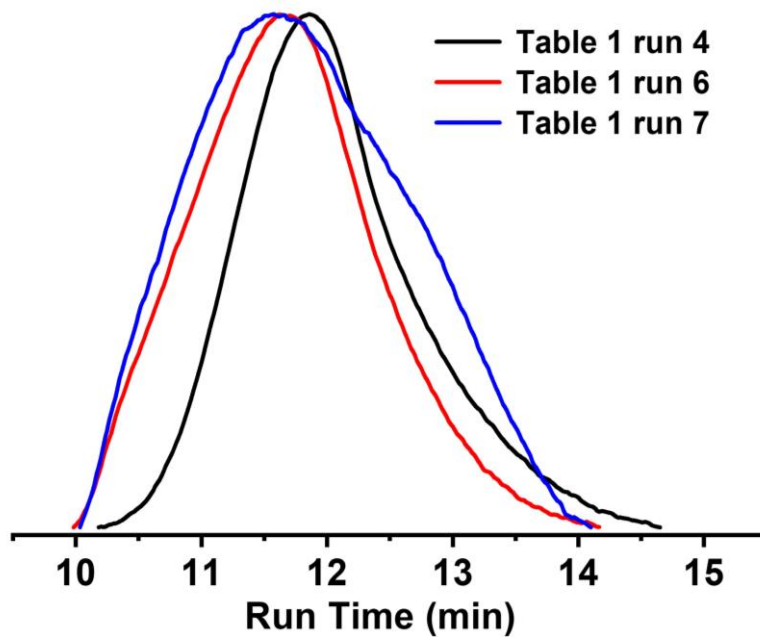


Fig. S19. GPC curves of polyethylene samples obtained in Table 1 runs 4, 6, and 7.

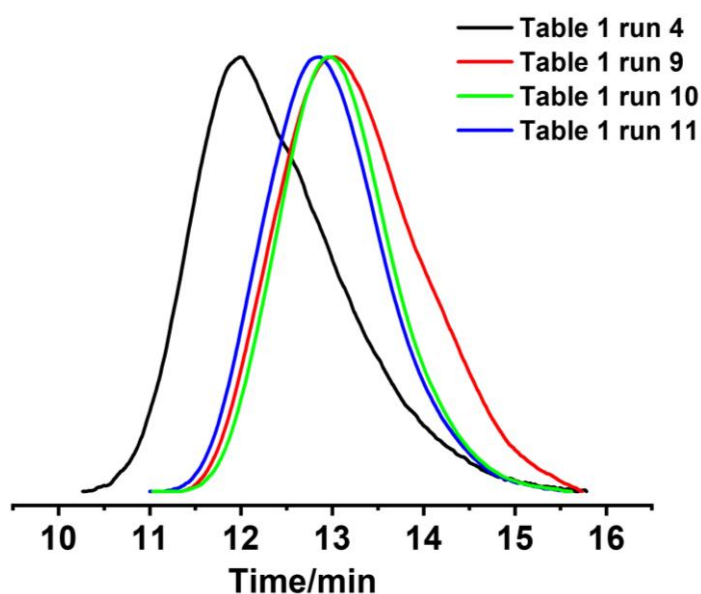


Fig. S20. GPC curves of polymers prepared by *syn-Hf₂*, *mono-Hf₁*, *Me-Hf₁* and *Ar-Hf₁* complexes under otherwise identical conditions (Table 1, runs 4, and 9–11).

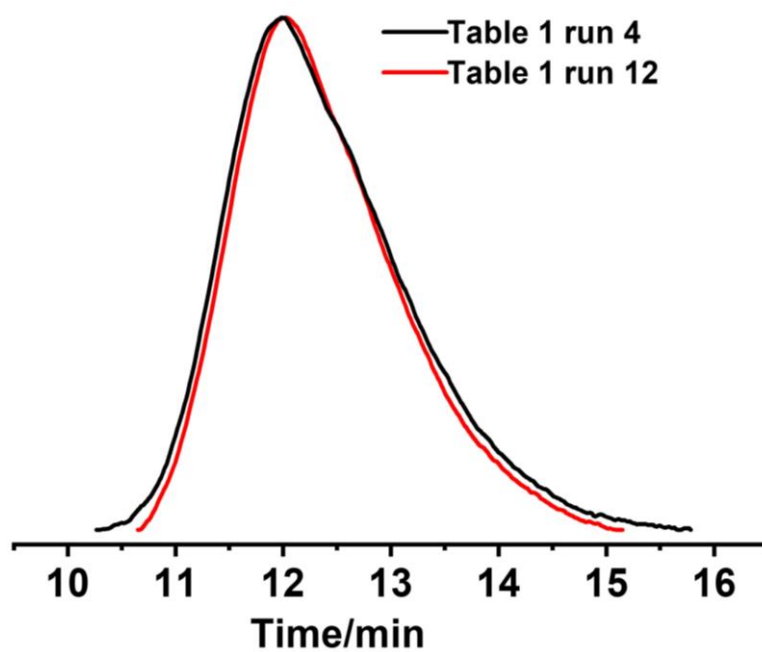


Fig. S21. GPC curves of polyethylene samples obtained in Table 1 runs 4 and 12.

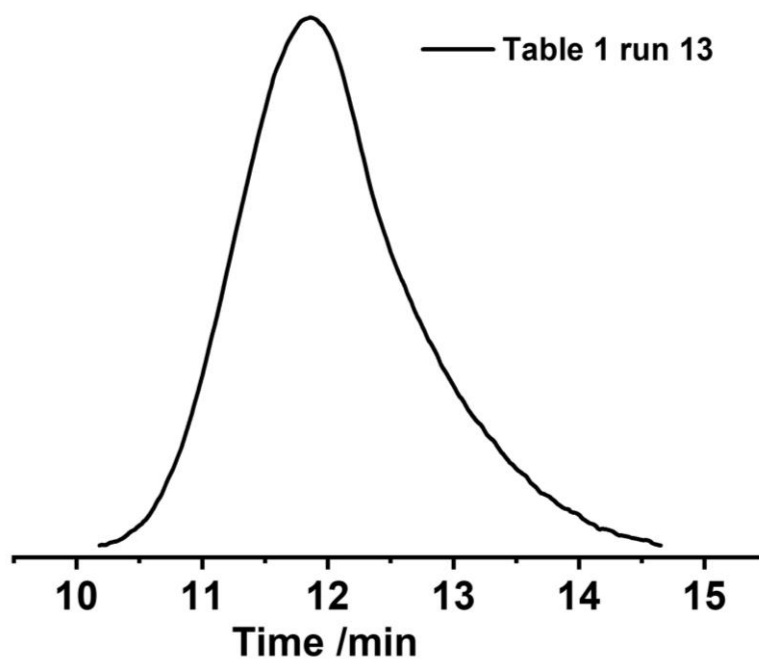


Fig. S22. GPC curve of polyethylene sample obtained in Table 1 run 13.

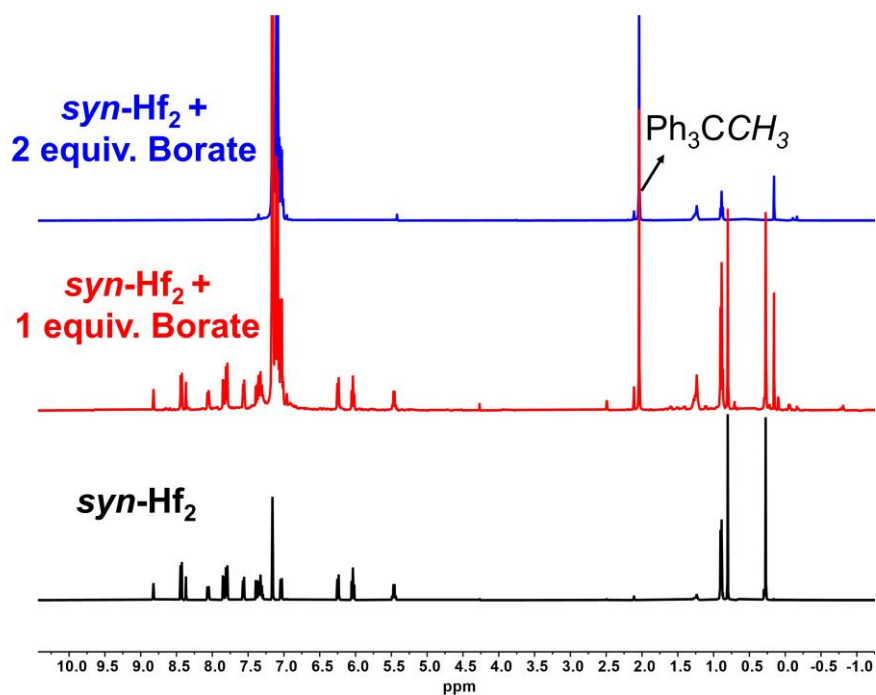


Fig. S23. Stacked ¹H NMR spectra of *syn*-Hf₂ (black), and *syn*-Hf₂ + 1 (red) or 2 (blue) equiv. of [Ph₃C][B(C₆F₅)₄] in C₆D₆.

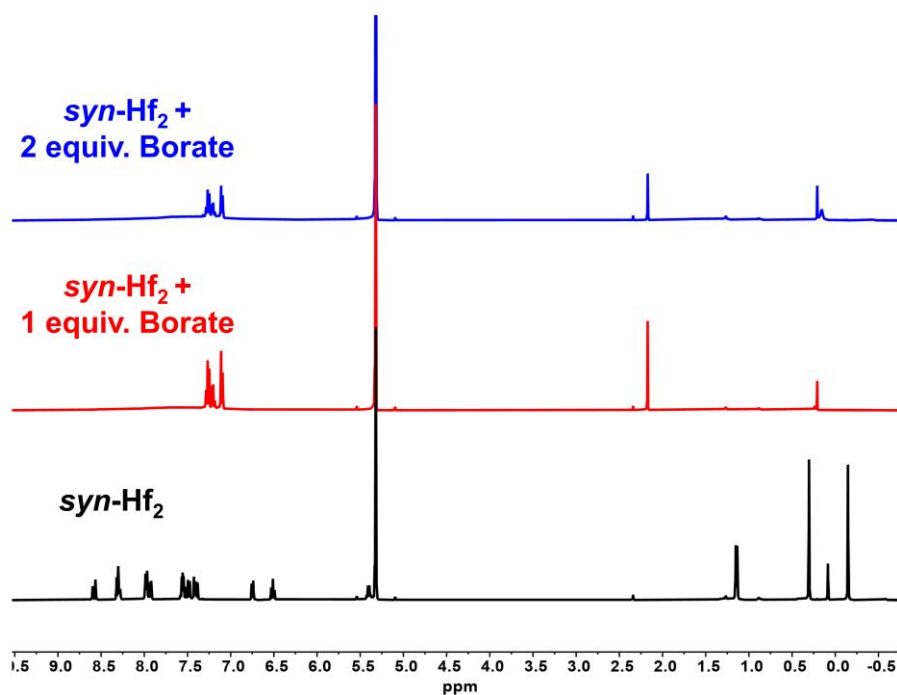


Fig. S24. Stacked ¹H NMR spectra of *syn*-Hf₂ (black), and *syn*-Hf₂ + 1 (red) or 2 (blue) equiv. of [Ph₃C][B(C₆F₅)₄] in CD₂Cl₂.

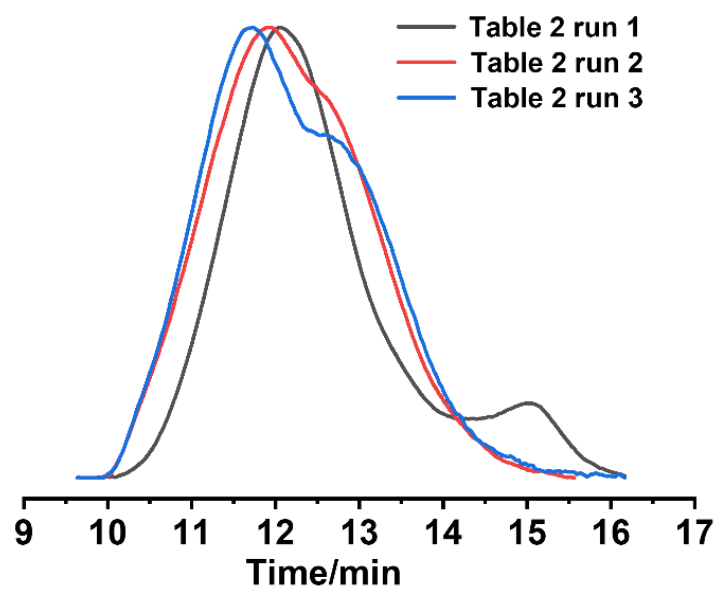


Fig. S25. GPC curves of ethylene/1-octene copolymer samples in Table 2 runs 1–3.

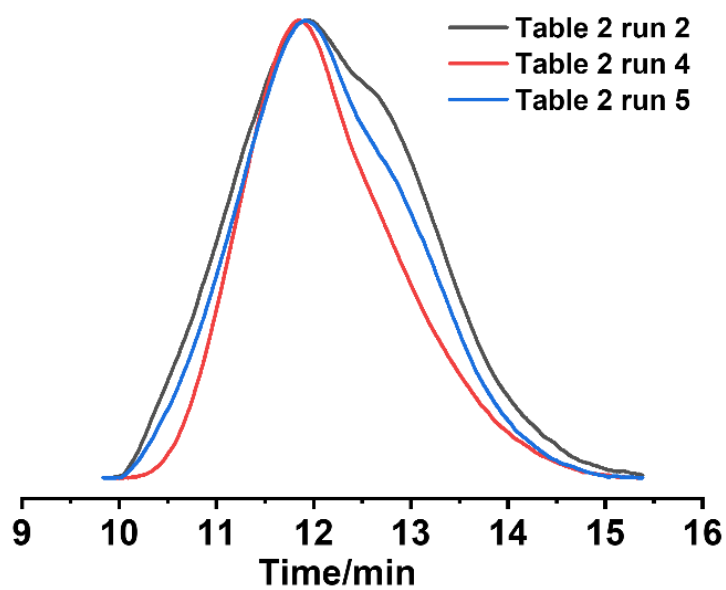


Fig. S26. GPC curves of ethylene/1-octene copolymer samples in Table 2 runs 2, 4, and 5.

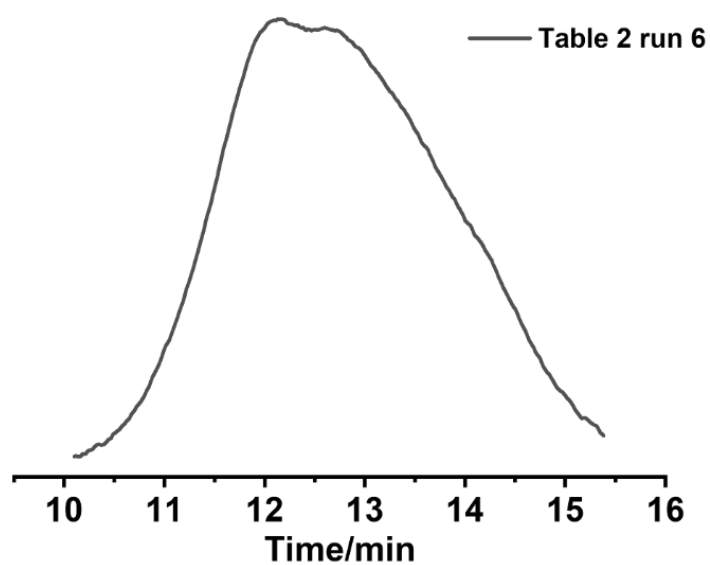


Fig. S27. GPC curve of ethylene/1-octene copolymer sample in Table 2 run 6.

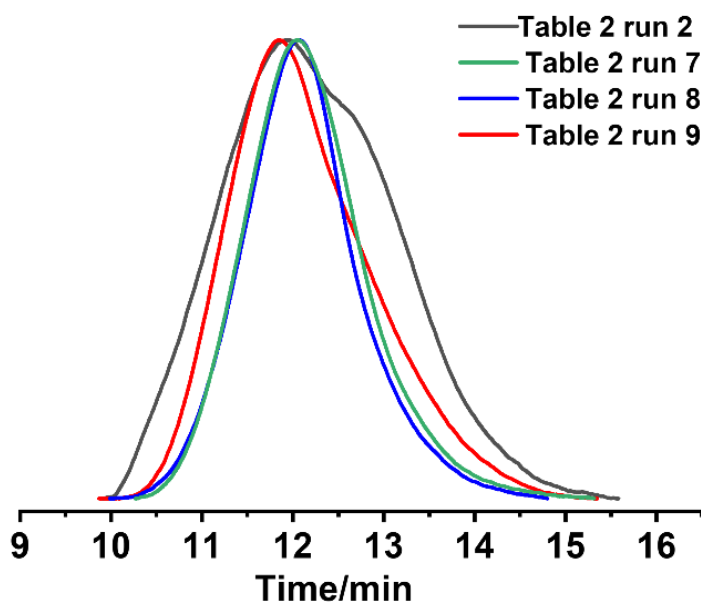


Fig. S28. GPC curves of ethylene/1-octene copolymer samples in Table 2 runs 2, and 7–9.

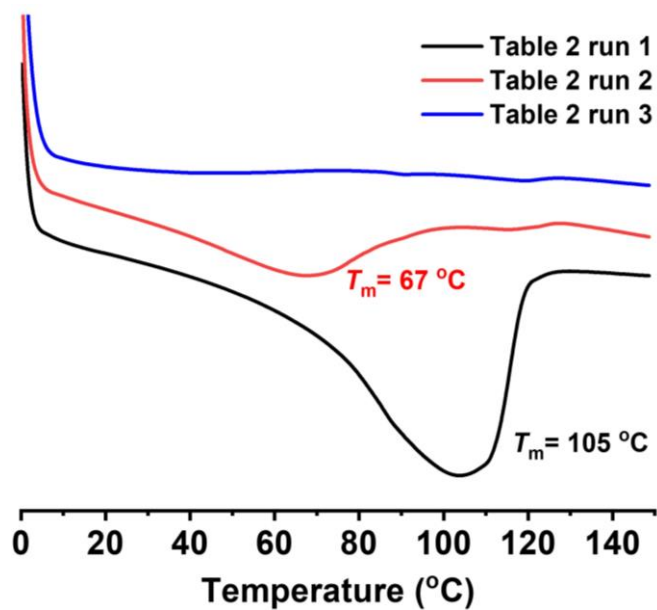


Fig. S29. DSC curves of ethylene/1-octene copolymer samples in Table 2 runs 1–3.

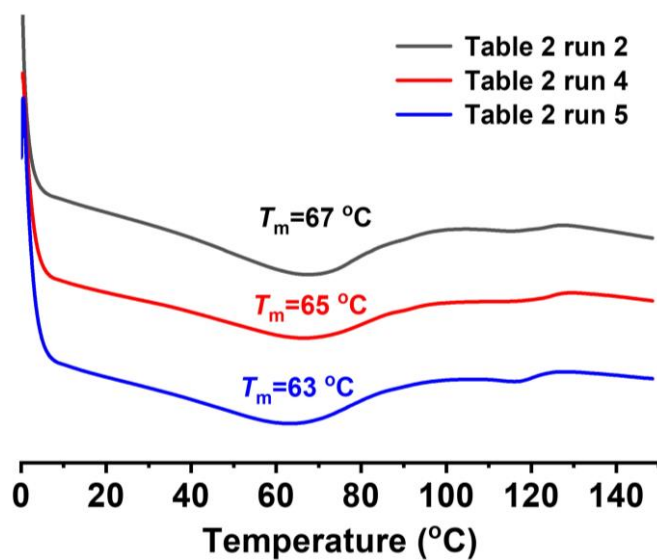


Fig. S30. DSC curves of ethylene/1-octene copolymer samples in Table 2 runs 2, 4 and 5.

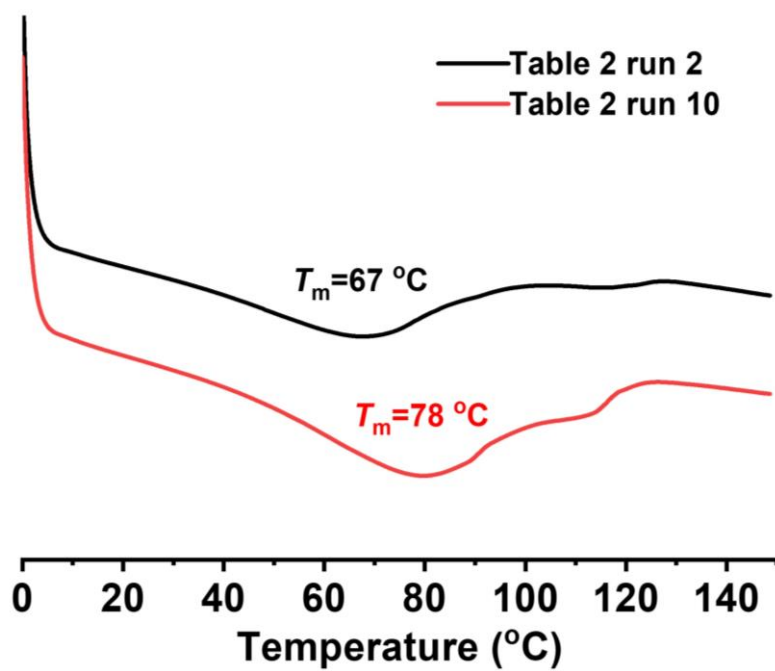


Fig. S31. DSC curves of ethylene/1-octene copolymer samples in Table 2 runs 2 and 10.

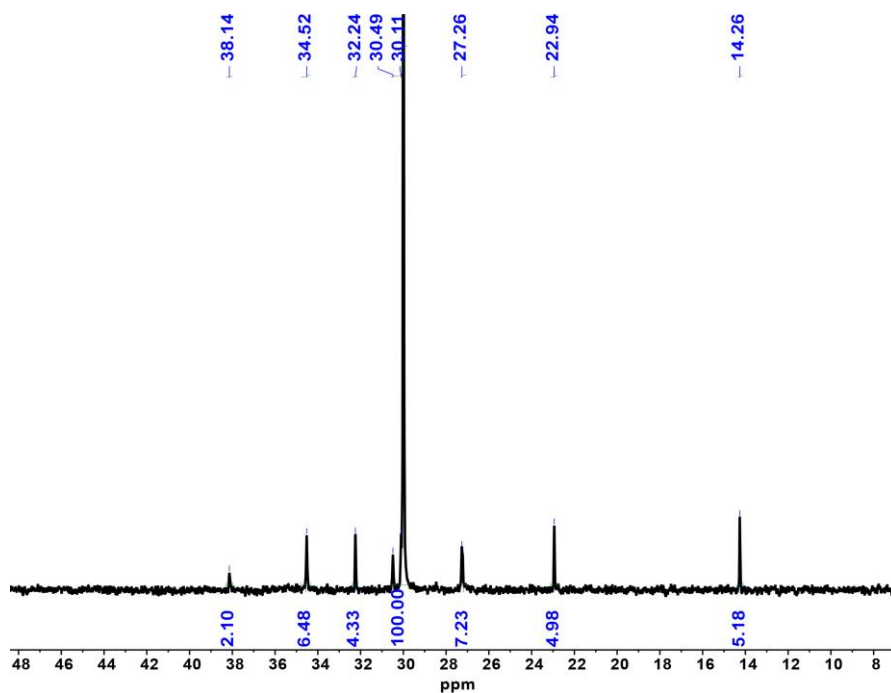


Fig. S32. ^{13}C NMR spectrum of ethylene/1-octene copolymer obtained in Table 2 run 1 in $\text{C}_2\text{D}_2\text{Cl}_4$ at $120\text{ }^\circ\text{C}$ (4.0 mol% of 1-octene incorporation).

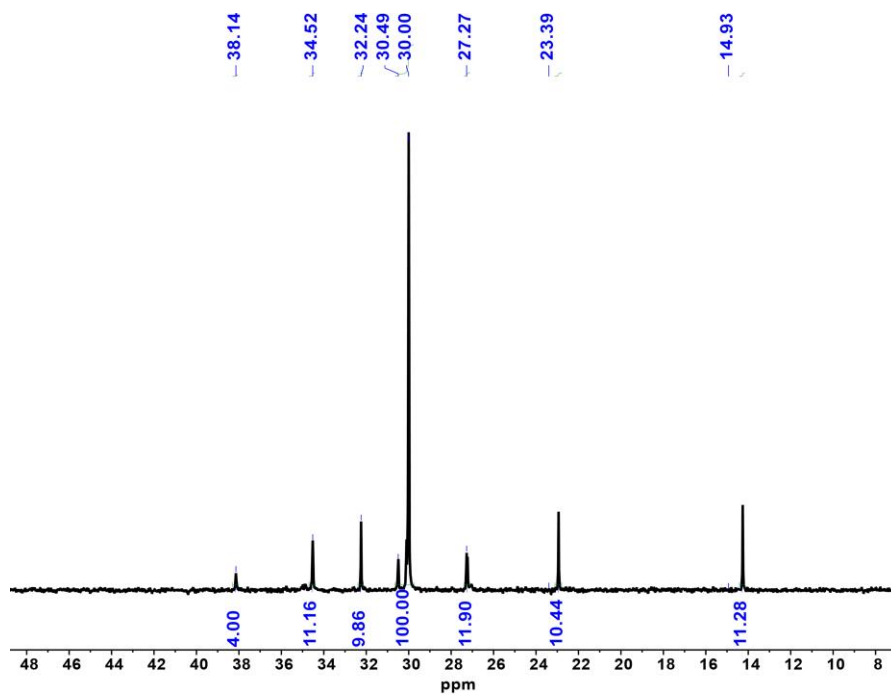


Fig. S33. ^{13}C NMR spectrum of ethylene/1-octene copolymer obtained in Table 2 run 2 in $\text{C}_2\text{D}_2\text{Cl}_4$ at $120\text{ }^\circ\text{C}$ (7.9 mol% of 1-octene incorporation).

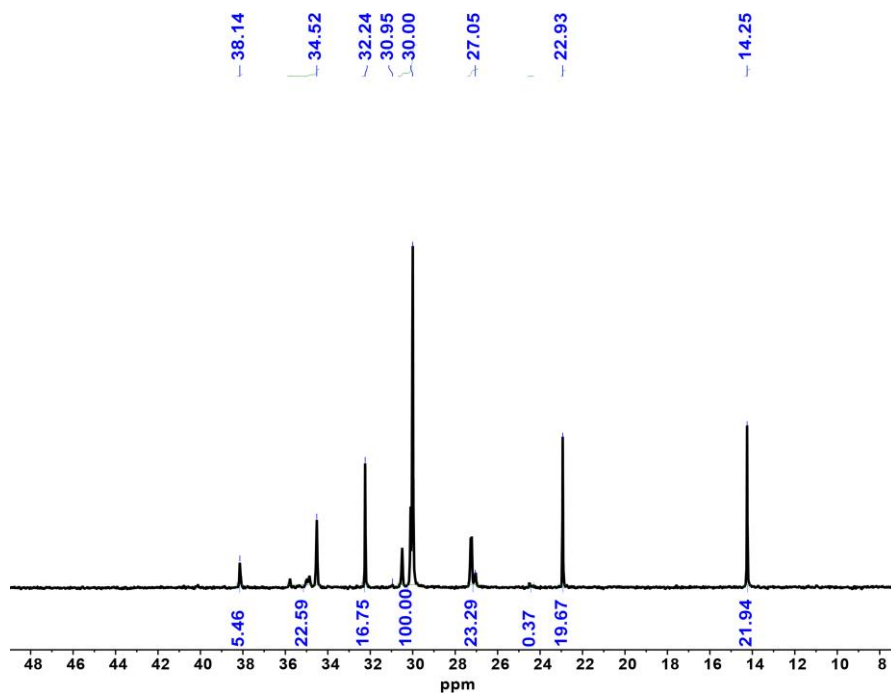


Fig. S34. ^{13}C NMR spectrum of ethylene/1-octene copolymer obtained in Table 2 run 3 in $\text{C}_2\text{D}_2\text{Cl}_4$ at $120\text{ }^\circ\text{C}$ (12.7 mol% of 1-octene incorporation).

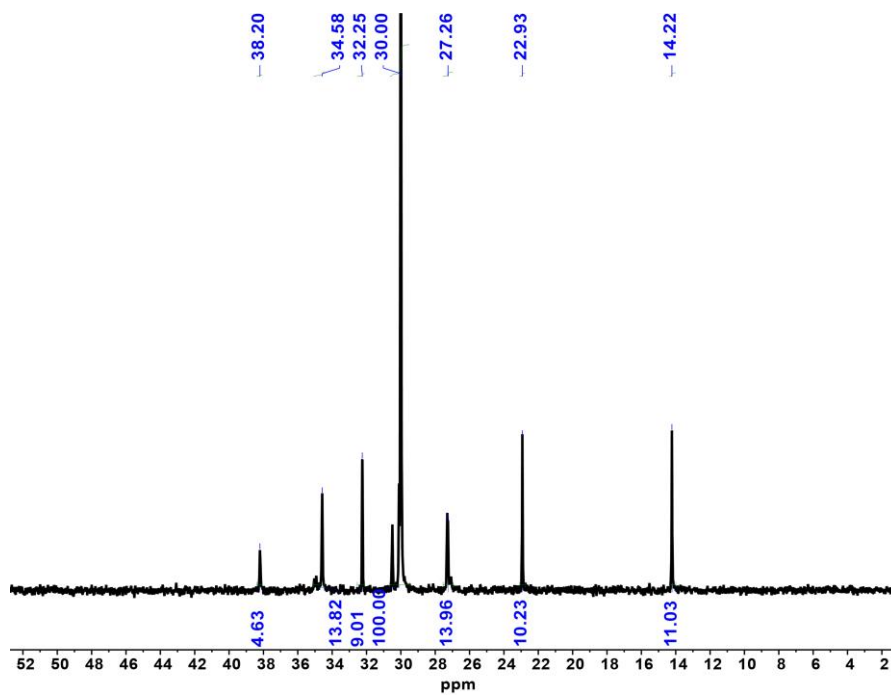


Fig. S35. ^{13}C NMR spectrum of ethylene/1-octene copolymer obtained in Table 2 run 4 in $\text{C}_2\text{D}_2\text{Cl}_4$ at $120\text{ }^\circ\text{C}$ (7.9 mol% of 1-octene incorporation).

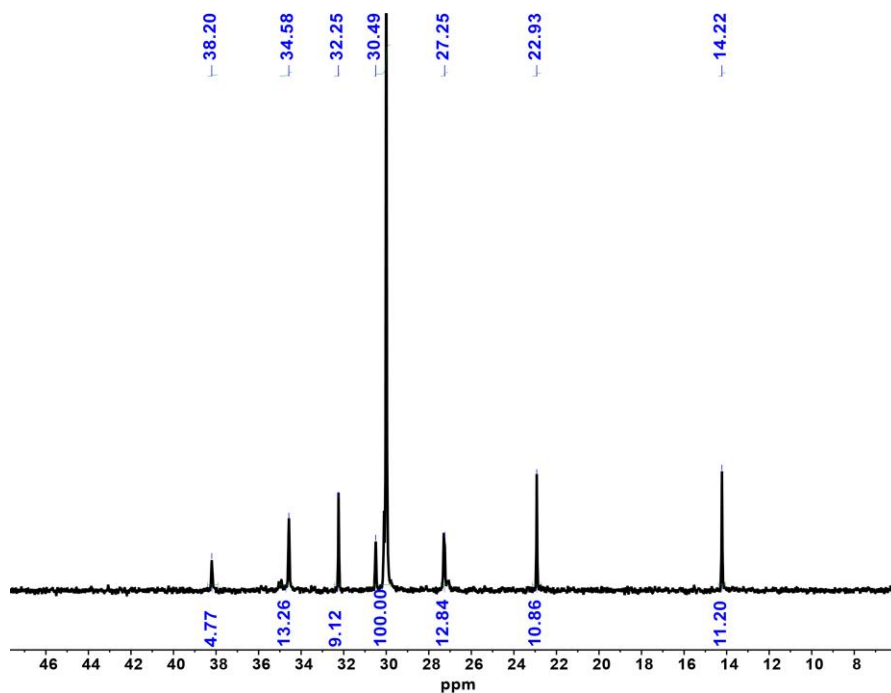


Fig. S36. ^{13}C NMR spectrum of ethylene/1-octene copolymer obtained in Table 2 run 5 in $\text{C}_2\text{D}_2\text{Cl}_4$ at $120\text{ }^\circ\text{C}$ (8.3 mol% of 1-octene incorporation).

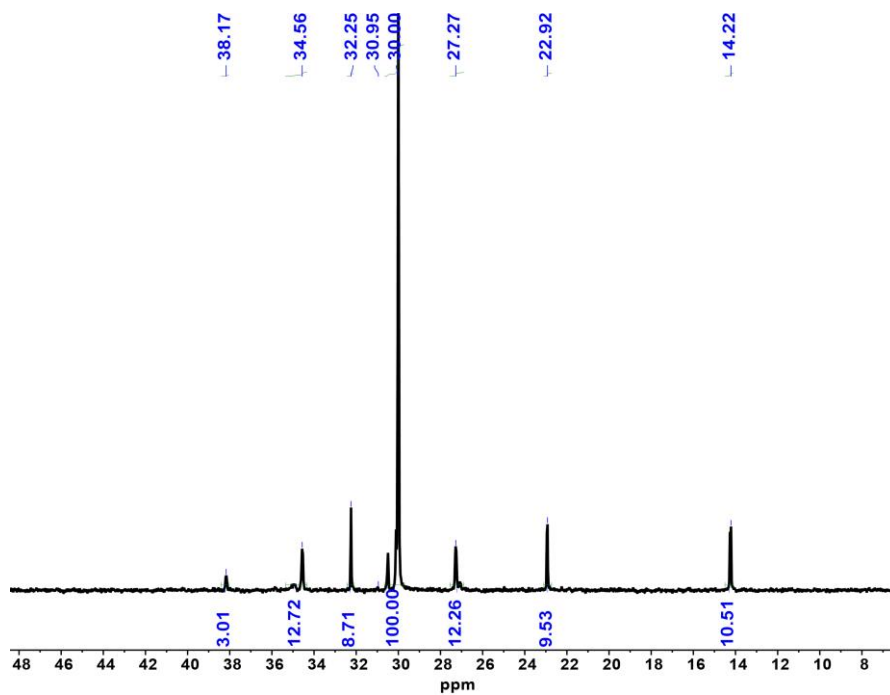


Fig. S37. ^{13}C NMR spectrum of ethylene/1-octene copolymer obtained in Table 2 run 6 in $\text{C}_2\text{D}_2\text{Cl}_4$ at $120\text{ }^\circ\text{C}$ (5.9 mol% of 1-octene incorporation).

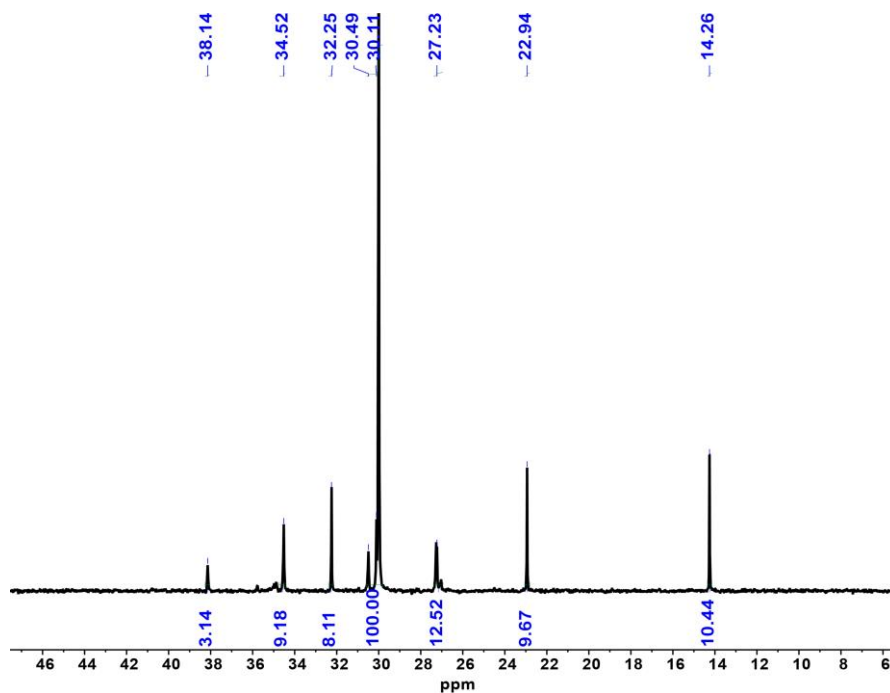


Fig. S38. ^{13}C NMR spectrum of ethylene/1-octene copolymer obtained in Table 2 run 7 in $\text{C}_2\text{D}_2\text{Cl}_4$ at $120\text{ }^\circ\text{C}$ (5.7 mol% of 1-octene incorporation).

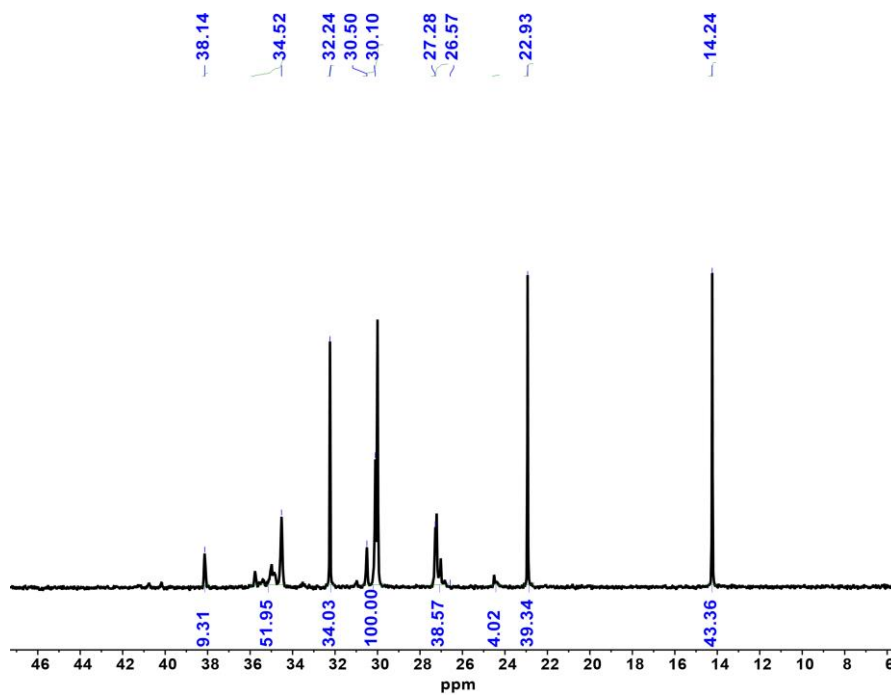


Fig. S39. ^{13}C NMR spectrum of ethylene/1-octene copolymer obtained in Table 2 run 8 in $\text{C}_2\text{D}_2\text{Cl}_4$ at 120 °C (32.9 mol% of 1-octene incorporation).

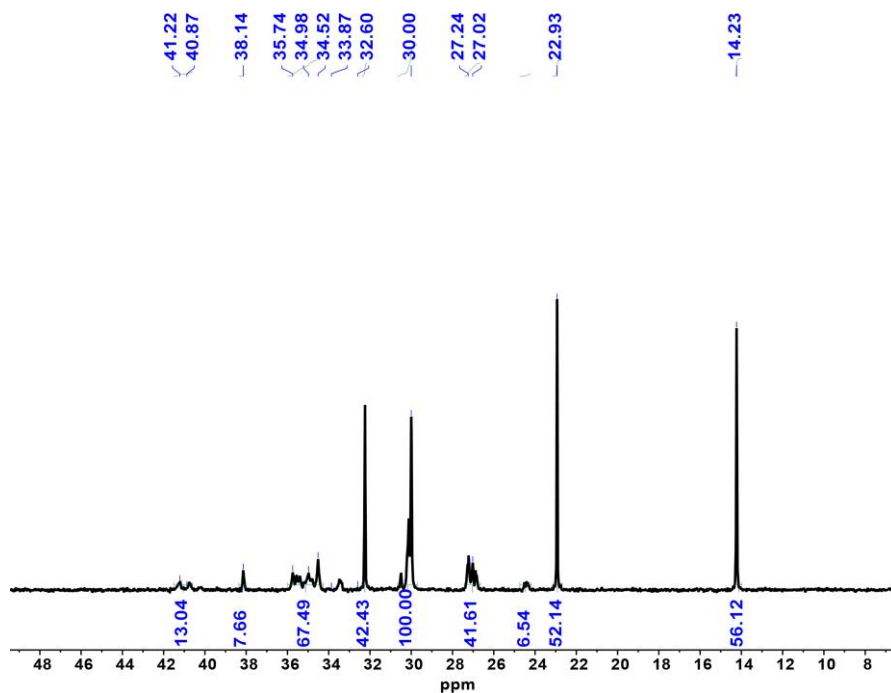


Fig. S40. ^{13}C NMR spectrum of ethylene/1-octene copolymer obtained in Table 2 run 9 in $\text{C}_2\text{D}_2\text{Cl}_4$ at 120 °C (37.4 mol% of 1-octene incorporation).

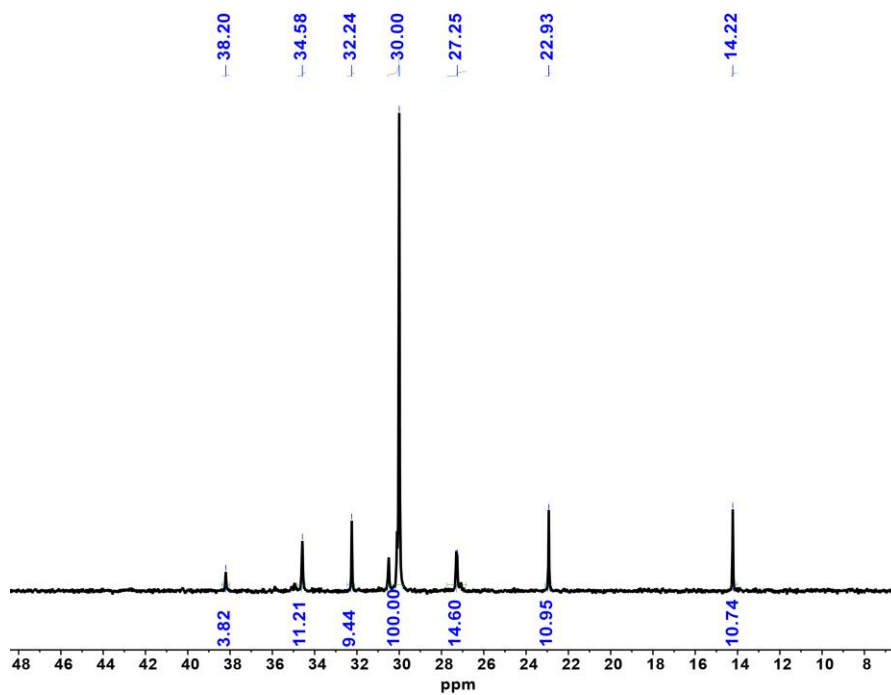


Fig. S41. ^{13}C NMR spectrum of ethylene/1-octene copolymer obtained in Table 2 run 10 in $\text{C}_2\text{D}_2\text{Cl}_4$ at 120 °C (6.6 mol% of 1-octene incorporation).

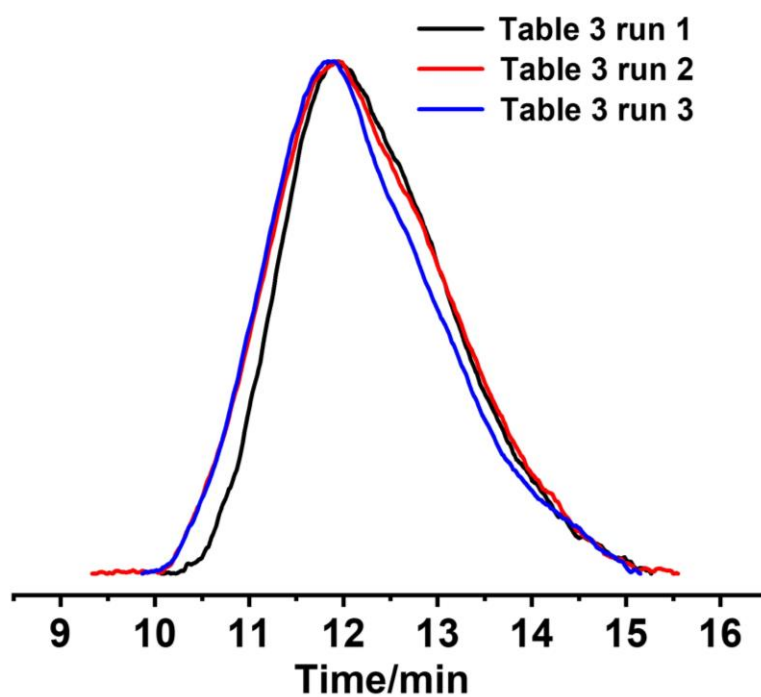


Fig. S42. GPC curves of polypropylene samples obtained in Table 3 runs 1–3.

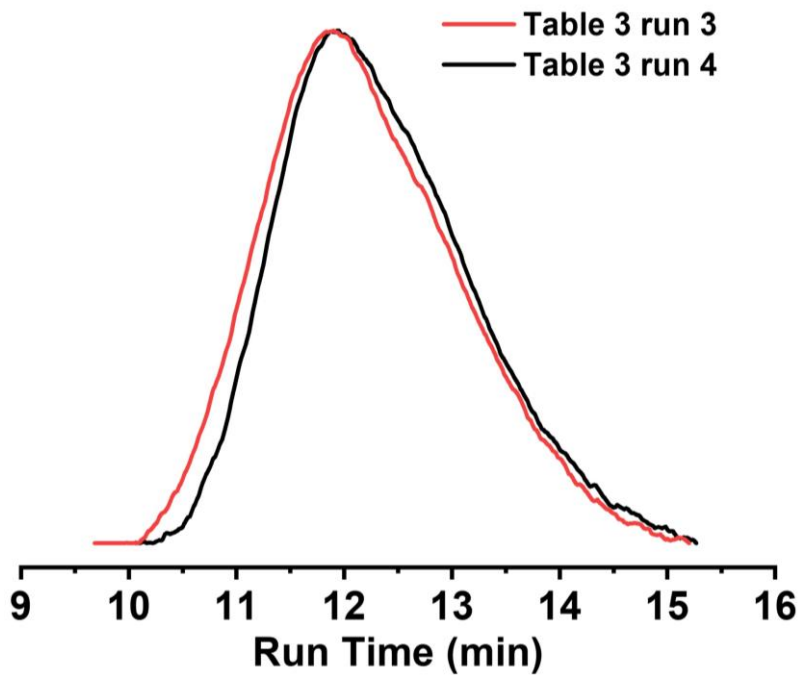


Fig. S43. GPC curves of polypropylene samples obtained in Table 3 runs 3 and 4.

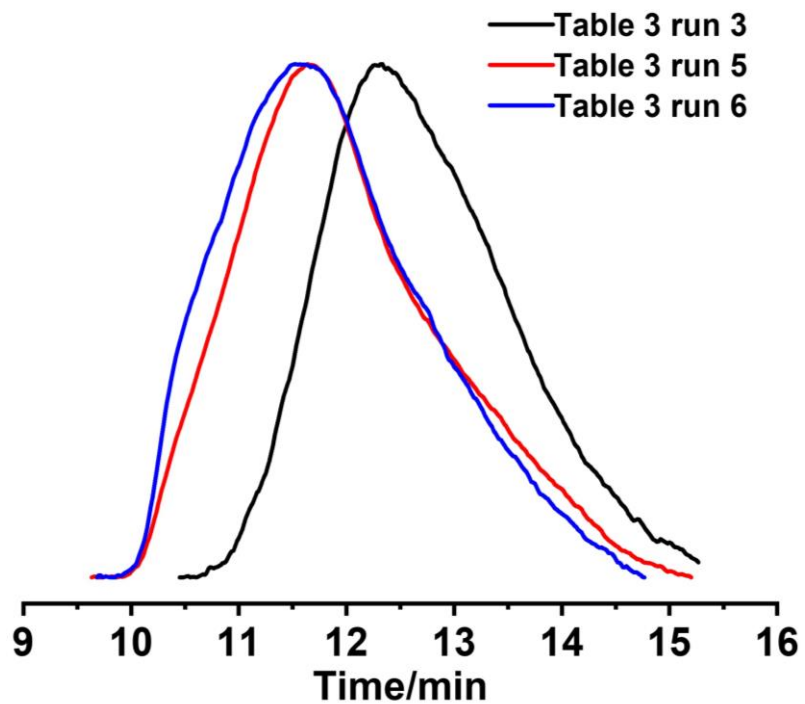


Fig. S44. GPC curves of polypropylene samples obtained in Table 3 runs 3, 5 and 6.

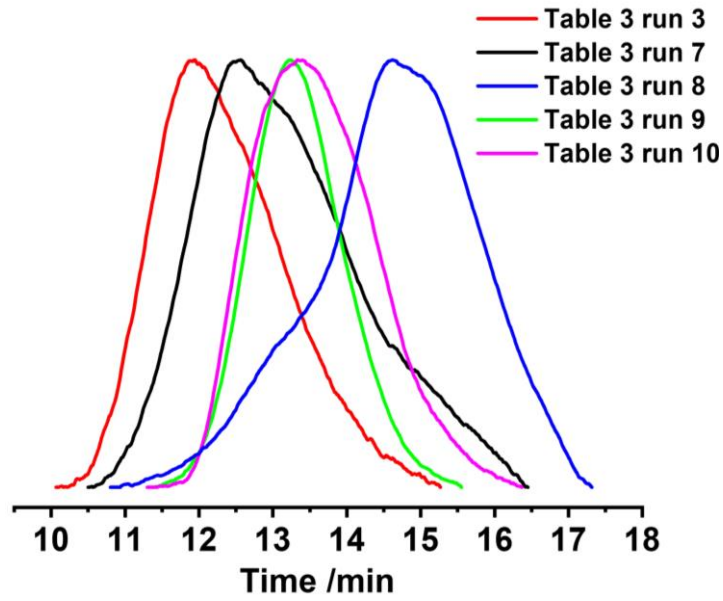


Fig. S45. GPC curves of polypropylene samples obtained in Table 3 runs 3, and 7–10.

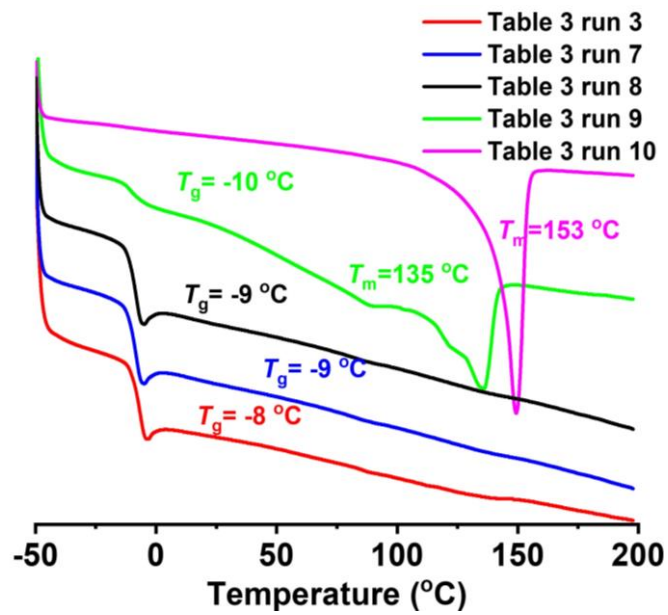


Fig. S46. DSC curves of propylene polymers obtained in Table 3 runs 3, and 7–10.

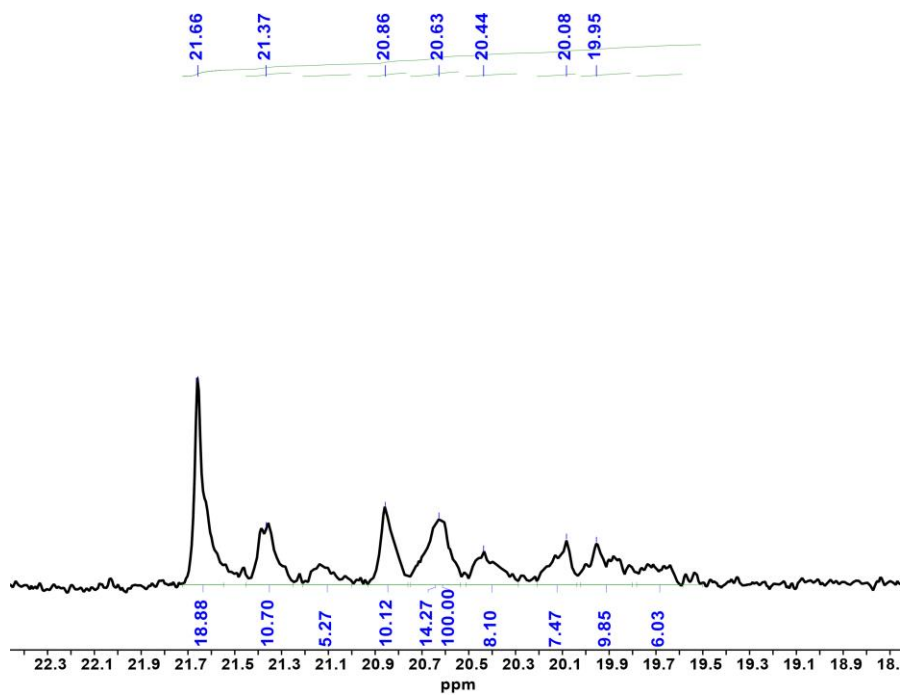


Fig. S47. ¹³C NMR spectrum of PP obtained in Table 3 run 3 in C₂D₂Cl₄ at 120 °C (18.8 *mmmm*%).

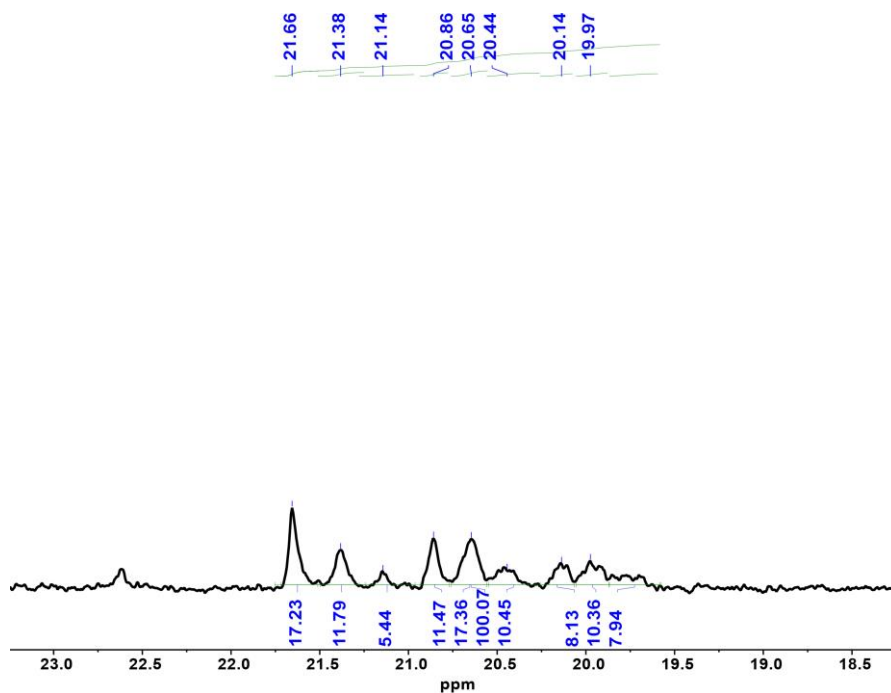


Fig. S48. ¹³C NMR spectrum of PP obtained in Table 3 run 4 in C₂D₂Cl₄ at 120 °C (17.2 *mmmm*%).

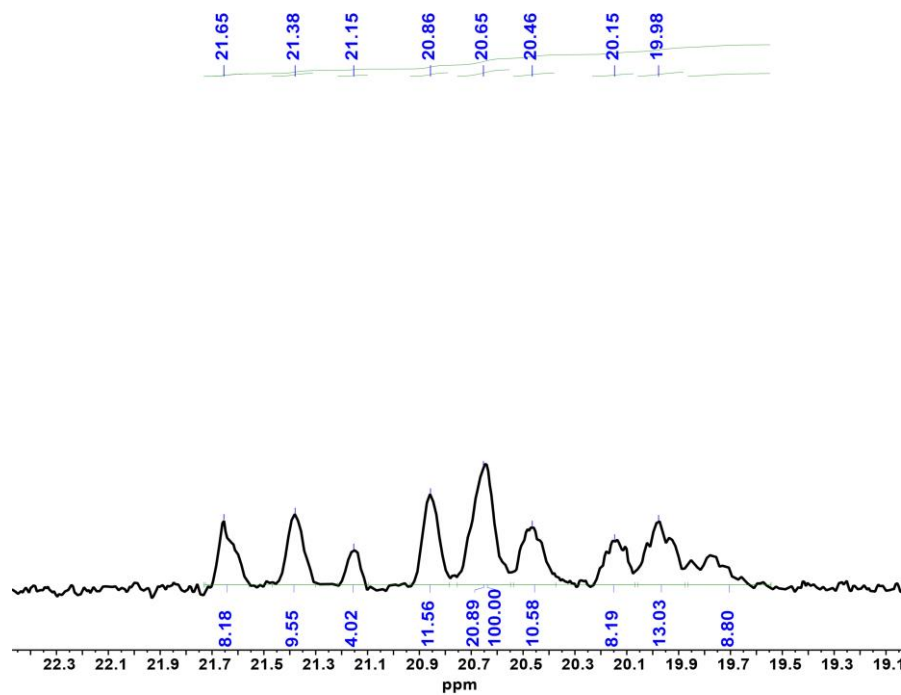


Fig. S49. ^{13}C NMR spectrum of PP obtained in Table 3 run 7 in $\text{C}_2\text{D}_2\text{Cl}_4$ at $120\text{ }^\circ\text{C}$ (8.2 *mmmm*%).

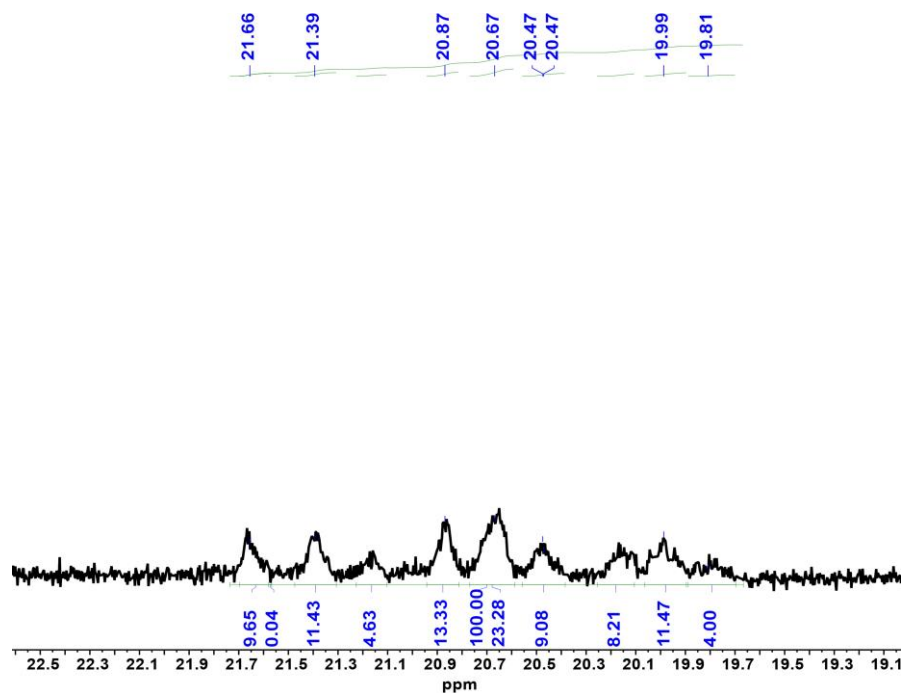


Fig. S50. ^{13}C NMR spectrum of PP obtained in Table 3 run 8 in $\text{C}_2\text{D}_2\text{Cl}_4$ at $120\text{ }^\circ\text{C}$ (9.6 *mmmm*%).

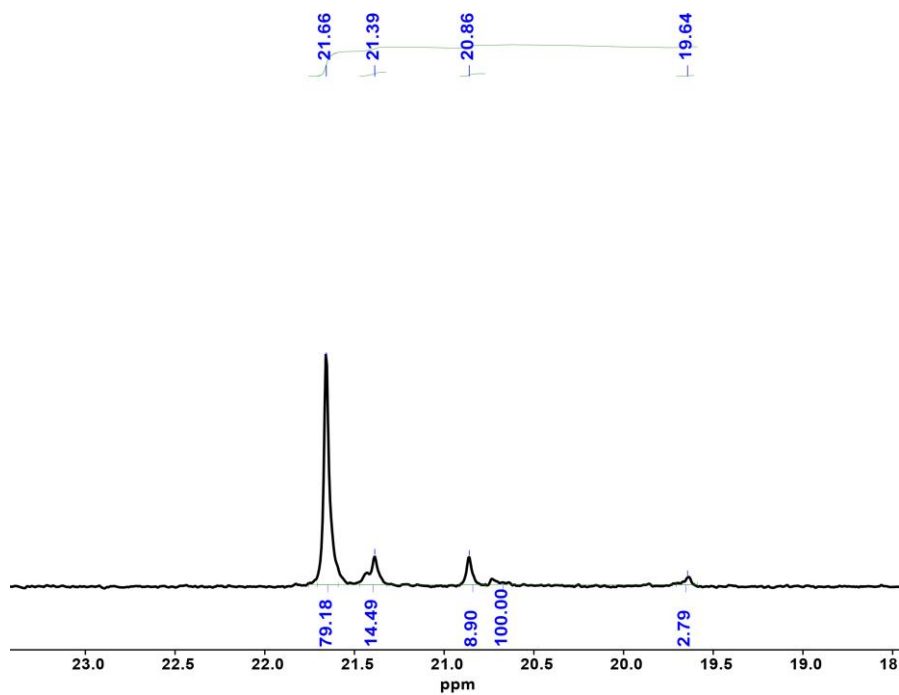


Fig. S51. ¹³C NMR spectrum of PP obtained in Table 3 run 9 in C₂D₂Cl₄ at 120 °C (79 *mmmm*%).

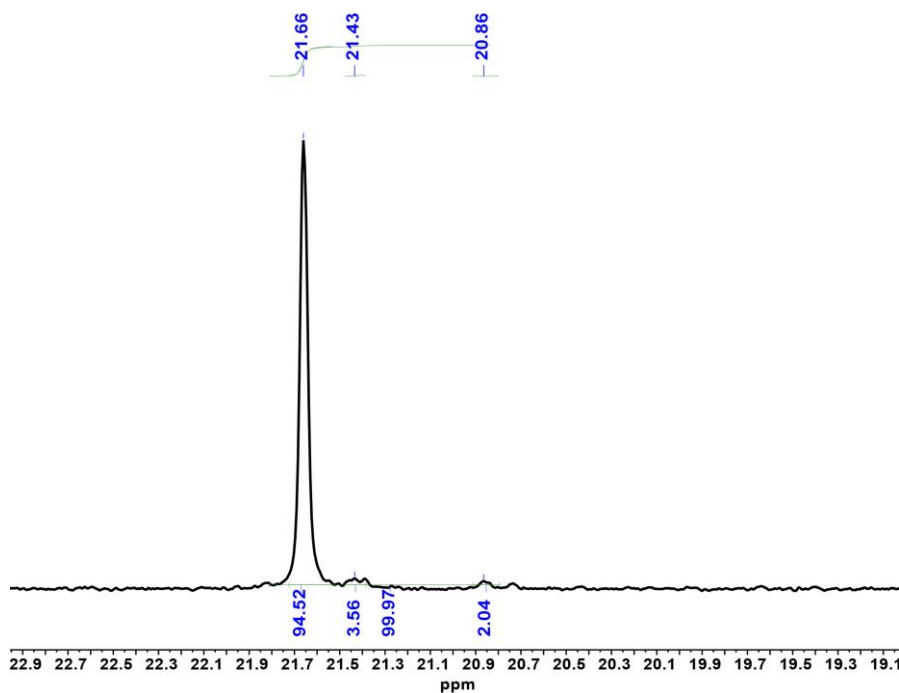


Fig. S52. ¹³C NMR spectrum of PP obtained in Table 3 run 10 in C₂D₂Cl₄ at 120 °C (94 *mmmm*%).

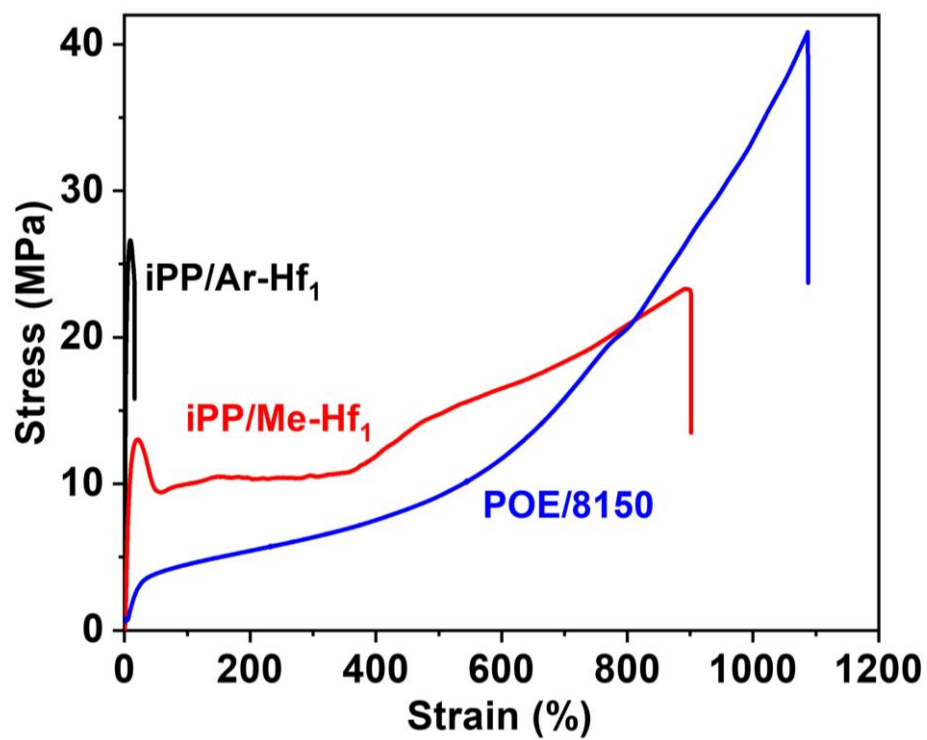


Fig. S53. Stress-Strain curve for commercial polyolefin elastomer sample (grade: POE/8150, blue) and iPP samples produced by **Ar-Hf₁** (black) and **Me-Hf₁** (red) at extension rate of 50 mm·min⁻¹.

Table S1. Pentad Distribution and Statistical Analysis for Polypropylene Obtained in Table 3.

PP Sample	Pentads(%)								
	<i>mmmm</i>	<i>mmmr</i>	<i>rmnr</i>	<i>mmrr</i>	<i>mrrm/rrmr</i>	<i>mrrr</i>	<i>rrrr</i>	<i>rrrrm</i>	<i>mrrm</i>
Table 3 run 3	18.88	10.70	5.27	10.12	14.27	8.10	7.47	9.85	6.03
Table 3 run 4	17.23	11.81	5.21	11.47	17.36	10.45	8.11	10.36	7.85
Table 3 run 7	8.18	9.55	4.02	11.56	20.89	10.58	8.19	13.03	8.80
Table 3 run 8	79.18	14.49	0	8.90	2.79	0	0	0	0
Table 3 run 9	94.52	3.56	0	0	2.04	0	0	0	0
Table 3 run 10	9.65	0.04	11.43	4.63	23.28	9.08	8.32	11.47	4.00

Table S2. Crystal Data and Structure Refinement for Metal Complex *syn-Hf₂*.

Complex	<i>syn-Hf₂</i>
Empirical formula	C ₆₆ H ₆₂ Hf ₂ N ₄
Formula weight	1268.17
Temperature / K	193.00
Crystal system	monoclinic
Space group	P2 ₁ /C
a / Å, b / Å, c / Å	17.6490(4), 12.8229(3), 24.5818(6)
α/°, β/°, γ/°	90, 101.2440(10), 90
Volume / Å ³	5456.4(2)
Z	4
ρ _{calc} / mg mm ⁻³	1.544
μ / mm ⁻¹	3.847
F(000)	2520.0
Crystal size / mm ³	0.18 × 0.15 × 0.12
Radiation	MoKα (λ = 0.71073)
2θ range for data collection	3.598 to 54.992
Index ranges	-22 ≤ h ≤ 22, -16 ≤ k ≤ 16, -31 ≤ l ≤ 28
Reflections collected	50389
Independent reflections	[R(int) = 0.0418]
Data/restraints/parameters	12503 / 210 / 698
Goodness-of-fit on F ²	1.035
Final R indexes [I > 2σ (I)]	R1 = 0.0283, wR2 = 0.0556
Final R indexes [all data]	R1 = 0.0410, wR2 = 0.0605
Largest diff. peak/hole / e Å ⁻³	0.90/ -0.55

Table S3. Mechanical Properties of PP samples Produced in Table 3.

Sample	M_w^a ($10^4 \text{ g}\cdot\text{mol}^{-1}$)	σ_b^b (MPa)	ϵ_b^b (%)	E_t^b (MPa)	Toughness ^b (MJ/m ³)	SR ^c (%)
aPP/ <i>syn</i> -Hf ₂	125	3.4±0.1	1055±35.4	3.0	16.8±1.4	87.6
aPP/ <i>syn</i> -Zr ₂	79	2.4±0.2	808±12.7	2.6	7.9±0.2	82.4
aPP/ <i>mono</i> -Hf ₁	10.5	1.3±0.1	653±22.6	2.2	7.1±0.3	78.2
iPP/Me-Hf ₁	16.2	21.8±0.1	870±16.7	118.4	130.3±2.3	14.6
iPP/Ar-Hf ₁	19.5	28.8±0.3	12.6±2.0	135.1	36.4±1.2	- ^e
POE/8150	- ^d	39.5±0.2	1049±24.2	10.5	150.2±2.4	47.4

^a Determined by GPC. ^b Tensile strength (σ_b), elongation at break (ϵ_b), Young's modulus (E_t) and toughness were determined by a universal testing instrument. ^c Hysteresis experiments for ten cycles at a strain of 200%. ^d Not determined. ^e Not observed.

References:

1. W. Liu, P. L. Rinaldi, L. H. McIntosh and R. P. Quirk, *Macromolecules*, 2001, **34**, 4757-4767.
2. V. Busico and R. Cipullo, *Prog. Polym. Sci.*, 2001, **26**, 443-533.
3. T. Shi, Q. Zheng, W. Zuo, S. Liu and Z. Li, *Chin. J. Polym. Sci.*, 2018, **36**, 149-156.
4. C. Feng, S. Zhou, D. Wang, Y. Zhao, S. Liu, Z. Li and P. Braunstein, *Organometallics*, 2021, **40**, 184-193.
5. T. R. Boussie, G. M. Diamond, C. Goh, K. A. Hall, A. M. LaPointe, M. K. Leclerc, V. Murphy, J. A. W. Shoemaker, H. Turner, R. K. Rosen, J. C. Stevens, F. Alfano, V. Busico, R. Cipullo and G. Talarico, *Angew. Chem., Int. Ed.*, 2006, **45**, 3278-3283.
6. K. A. Frazier, R. D. Froese, Y. He, J. Klosin, C. N. Theriault, P. C. Vosejka, Z. Zhou and K. A. Abboud, *Organometallics*, 2011, **30**, 3318-3329.
7. G. M. Sheldrick, *Acta Crystallogr., Sect. C: Struct. Chem.*, 2015, **C71**, 3-8.